Comparison of the ultra-low-dose Veo algorithm with the gold standard filtered back projection for detecting pulmonary asbestos-related conditions

Journal:	*BMJ Open*
Manuscript ID:	bmjopen-2014-004980
Article Type:	Research
Date Submitted by the Author:	01-Feb-2014
Complete List of Authors:	Tekath, Marielle; University Hospital CHU Clermont-Ferrand, Dutheil, Frederic; CHU G Montpied, Occupational Medicine Bellini, Romain Roche, Antoine; University Hospital CHU Clermont-Ferrand, Pereira, Bruno; University Hospital CHU Clermont-Ferrand, Naughton, Geraldine; Australian Catholic University, School of Exercise Science Chamoux, Alain; CHU G. Montpied, Occupational Medicine Michel, Jean-Luc; University Hospital CHU Clermont-Ferrand,
Primary Subject Heading:	Occupational and environmental medicine
Secondary Subject Heading:	Radiology and imaging, Public health
Keywords:	OCCUPATIONAL & INDUSTRIAL MEDICINE, Computed tomography < RADIOLOGY & IMAGING, PUBLIC HEALTH

Comparison of the ultra-low-dose *Veo* algorithm with the gold standard filtered back projection for detecting pulmonary asbestos-related conditions

Marielle Tekath[1], Frédéric Dutheil[2,3,4,5], Romain Bellini[6], Antoine Roche[1], Bruno Pereira[7], Geraldine Naughton[3,*], Alain Chamoux[2], Jean-Luc Michel[1]

[1] Department of Radiology, University Hospital CHU G. Montpied, Clermont-Ferrand, France

[2] Occupational Medicine, University Hospital CHU G. Montpied, Clermont-Ferrand, France

[3] School of Exercise Science, Australian Catholic University, Locked Bag 4115, Fitzroy MDC, VIC 3065, Australia

[4] Laboratory of Metabolic Adaptations to Exercise in Physiological and Pathological conditions EA3533, Blaise Pascal University, Clermont-Ferrand, France

[5] INRA, UMR 1019, UNH, CRNH Auvergne, Clermont-Ferrand, France

[6] Department of Radiology, Centre Jean Perrin, University Hospital CHU Clermont-Ferrand, France

[7] Department of Medical Statistics, University Hospital CHU G. Montpied, Clermont-Ferrand, France

*** Correspondance to**: Geraldine Naughton; Geraldine.Naughton@acu.edu.au

Running title: *Veo* in asbestos-related conditions

Words count for introduction methods results discussion and conclusion: 2946

Number of tables: 3

Number of figures: 2

Words count for abstract: 249

ABSTRACT

Objectives: Radiation delivered during computed tomography is a major concern, especially for individuals undergoing repeated screening. We aimed to compare a new ultra-low dose algorithm called *Veo* with the gold standard filtered back projection (FBP) for detecting pulmonary asbestos-related conditions.

Setting: University Hospital CHU G. Montpied, Clermont-Ferrand, France

Participants: Asbestos-exposed workers were recruited following referral to screening for asbestos-related conditions. Two acquisitions were performed on a 64-slice computed tomography: the gold standard FBP followed by *Veo* reconstruction.

Outcome measures: Two radiologists independently assessed asbestos-related abnormalities, pulmonary nodules, radiation doses, and image quality (noise).

Results: We included 27 asbestos-exposed workers (63.3±6.5 years with 11.9±9.7 years of asbestos-exposure). We observed 297 pleural plaques in 20 participants (74%). All patients (100%) had pulmonary nodules, totaling 167 nodules. Detection rates did not differ for pleural plaques (*Veo* 87% vs. FBP 97%, NS), pleural thickening (100% for both) and pulmonary nodules (80% for both). Interstitial abnormalities were depicted less frequently with *Veo* than FBP. False negative and false positive did not exceed 2.7%. Compared with FBP, *Veo* decreased the radiation dose up to 87% (*Veo* 0.23±0.07 vs. FBP 1.83±0.88 mSv, p<0.001). The objective image noise also decreased with *Veo* as much as 23% and signal to noise ratio increased up to 33%.

Conclusion: A low dose computed tomography with *Veo* reconstruction substantially reduced radiation. *Veo* compared favorably with FBP in detecting pleural plaques, pleural thickening and pulmonary nodules. However, due to a few false positives and false negatives, *Veo* may be better for following-up patients after initial screening with FBP (ClinicalTrials.gov number: NCT01955018).

Keywords computed tomography, radiation, screening, asbestos, workers, cancer

Strengths and limitations of this study

- Radiation delivered during computed tomography is a major concern, especially for individuals undergoing repeated screening, such as asbestos-exposed workers.
- We provides the first comparison of a new ultra-low dose algorithm called *Veo* ("I see" in Spanish) with the gold standard filtered back projection (FBP) in detecting pulmonary conditions in asbestos-exposed workers.
- *Veo* substantially reduces radiation doses, with 87% less radiation delivered than FBP.
- *Veo* compared favorably with FBP acquisitions in detecting pleural plaques, diffuse pleural thickening and pulmonary nodules; however, due to a few false positives and false negatives, *Veo* may be better for following-up asbestos-exposed workers after initial screening with FBP.
- Even if the sample size could be perceived as a limitation, the high prevalence of pleural plaques (297, observed in 74% of participants) and pulmonary nodules (167) permitted a robust statistical analysis.

INTRODUCTION

Asbestos fibers were intensively used throughout the 20th century [1], and remain prevalent in developing countries.[1] However, asbestos exposure induces a variety of benign and malignant pleural and lung diseases.[2 3] Due to a long latency period between exposure and disease presentation, asbestos-related diseases remain a substantial public health problem.[1] The most common asbestos-induced neoplasm is lung cancer.[2 3] Chest computed tomography (CT) screening has been successfully used in the early detection of lung cancer in asbestos-exposed workers.[4-6] Moreover, thin-section CT is more sensitive than a chest x-ray for detecting early asbestos-related conditions.[7-10] Nevertheless, the use of CT has two main disadvantages: high radiation doses and depiction of incidental abnormalities such as pulmonary nodules in asymptomatic patients. Incidental abnormalities increase the frequency of follow-up by CT and may also psychologically impact on patients. Medical exposure from x-rays represents the major source of man-made irradiation with a large contribution from CT.[11-13] Increased exposure to radiation underpins the consequences of cancer induction.[14] However, reducing CT doses increases image noise from the filtered back projection (FBP) reconstruction. Strategies to reduce radiation exposure include the use of iterative reconstruction algorithms such as “iDose”, “100% ASIR” and “IRIS”.[15-20] The new algorithm called *Veo*™ (General Electric Healthcare, Milwaukee, MI, USA) decreases the image noise up to 70% compared with the gold standard FBP model, whereas the “100% ASIR” algorithm is only capable of reducing image noise up to 47%.[21] Moreover, *Veo* (“I see” in Spanish) improves spatial resolution with excellent detection of low and high contrast objects from a CT Dose Index ($CTDI_{vol}$) equal to 0.3 mGy.

Thus, the objective of the present study was to compare *Veo* with the gold standard FBP for detecting pulmonary asbestos-related conditions among workers previously exposed to asbestos. Comparisons included radiation delivered and image quality.

METHODS

Patients

Our prospective clinical study received approval from the ethical committee of the University Hospital of Clermont-Ferrand (ClinicalTrials.gov number: NCT01955018). Written informed consent was obtained from all participants for the supplementary acquisition of *Veo* images in addition to their clinically indicated chest CT. Asbestos-exposed workers were recruited following referral to our radiology department for the evaluation of asbestos-related disease between September 2012, and April 2013. Inclusion criteria were being an asbestos-exposed workers, having a chest CT referral from the occupational medicine department, no history of cancer or thoracic surgery, and the absence of other known interstitial pathology.

CT protocol

CT examinations were performed with a 64-slice CT system (Discovery CT 750HD; GE Healthcare, Milwaukee, WI) and consisted of two successive acquisitions. Each examination, the normal-dose (FBP acquisition) and ultra-low-dose (*Veo* acquisition) spiral CT, was obtained on the entire thorax, at full inspiration with the participant in the supine position. No intravenous contrast material was administered. In accordance with guidelines, standard acquisition was performed with CT parameters adjusted to the participant's body size, including a tube kilovoltage (kV) of 120 (participants weighing 70 kg or less) and 140 (participants weighing more than 70 kg), with milliamperage (mA) equal to the patient's body weight. The other CT parameters were rotation time 0.5 s and pitch 1.375. Image data were reconstructed with FBP algorithm. The *Veo* acquisition was performed with constant CT

parameters including: a tube voltage of 100 kV, a tube current of 20 mA, pitch of 0.984 and rotation time 0.4 s. Image data were reconstructed with the *Veo* algorithm.

Interpretation of CT Images

Each CT acquisition was viewed independently by two experienced radiologists (2 to 7 years of experience). The low-dose images with *Veo* reconstruction were interpreted before the standard CT and on separate weeks to minimize recall bias. The gold standard CT was established by a second and simultaneous reading of the *Veo* and FBP acquisitions by the more experienced radiologist to evaluate the detection and characterization of pleuroparenchymal abnormalities. Because FBP images are benchmark practice, when a lesion was found only on *Veo* images, it was regarded as a false positive.

Pleural and parenchymal abnormalities

According to established criteria,[9 22 23] the following asbestos-related pleural and parenchymal abnormalities were recorded as present or absent. Pleural abnormalities considered were:

- Pleural plaques: pleura thickening with no associated parenchymal abnormality. We recorded for each lesion: localization (side, region: anterolateral, posterolateral, diaphragmatic or mediastinum), thickness, and calcification.

- Diffuse pleural thickening: pleural thickening associated with parenchymal abnormalities such as rounded atelectasis and parenchymal bands.[22]

- Pleural effusion is typically asymptomatic, the fluid may be serous or hemorrhagic.[22]

CT features of asbestosis included: 1) subpleural dots and branching opacities, 2) curvilinear subpleural lines, defined as linear opacity within 1 cm of the pleura and parallel to the inner chest wall, 3) areas of ground glass opacities, 4) septal lines and 5) reticulations defined as

single or branching lines 1-2 cm in length in the subpleural parenchyma, 6) honeycombing, defined as cystic air spaces with well-defined walls less than 1 cm diameter.

Presence of nodules was also recorded. We noted for each abnormality: localization (side, table position) and nature (non-solid, part-solid, solid or calcified). To increase sensitivity, nodules were examined by combining maximum intensity projections and millimetric axial CT images.[24]

Radiation

Comparisons included the dose length product (DLP) in mGy.cm and effective doses in mSv. Computed conversion factor from DLP to effective dose for adult chest is 0.0146 $mSv.mGy^{-1}.cm^{-1}$ [25].

Quality of FBP and *Veo* Images

Respiratory artifacts were graded on a three-point scale (1 = negligible, 2 = moderate, 3 = salient). Images noise was studied in the axial and coronal planes. A similar scale was used for subjective image quality in the mediastinum and parenchyma windows. Objective image noise (Standard Deviation) and average CT numbers (in Hounsfield's units) were measured with circular regions of interest (ROI) on different anatomical levels, 10 mm in diameter.[19] ROIs were drawn within the descending thoracic aorta at the level of the left main bronchus, within the tracheal lumen up to the tracheal bifurcation, and on the lung. The signal to noise ratio (SNR) was also calculated using the equation SNR = CT numbers / noise.[26]

Statistical Analysis

Sample size estimation was based on the number of pleural plaques and nodules. Considering the investigative nature of the study design and because the number of pleural plaques and

nodules was not known initially, a sample size estimation was not proposed *a priori* even though a concordance coefficient kappa (κ) between 0.40 and 0.90 was expected between filtered back projection images and *Veo* images. Therefore, 30 asbestos-exposed workers were predicted to be necessary to reject the null hypothesis "H0: $\kappa = 0.40$" vs. "H1: $\kappa \neq 0.75$" for a proportion of pleural plaques of 65%, with a statistical power of > 85% and α=5% (two-sided). Finally, the study was conducted to sequentially control the statistical power considering the number of plaques and nodules for each asbestos-exposed worker.[27]

Statistical analysis was performed using Stata software (version 12; Stata-Corp, College Station, Tex., USA). Quantitative variables are expressed as means ± standard deviations (SD). Proportions are expressed as percentage and 95% confidence intervals (CIs). Comparisons in paired situation were realized using paired Student t-test or Wilcoxon test when appropriate for quantitative variables and Stuart-Maxwell test for categorical parameters. Sensitivity, specificity, false positives and false negatives values of *Veo* were calculated and presented with 95% confidence intervals, in comparison with results from FBP acquisitions. Estimates of sensitivity and specificity were obtained by first estimating the sensitivity and specificity for each patient. Sensitivity and specificity were then estimated by averaging the individual specific estimates across patients. The variance of the estimate was the sample variance divided by the number of patients. General estimated equation models with logit link and working independence correlation structure were also used to estimate sensitivity, taking into account the correlation among the multiple pleural plaques and pulmonary nodules for the same patient. The kappa coefficient was used to measure agreement for categorical parameters and Pearson's correlation coefficient and Lin concordance correlation coefficient for quantitative data. The analyses were completed by using of random-effect models when appropriate to consider within and between participant variability. The tests were two-sided, with a type I error set at α=0.05.

RESULTS

Patients

The flow chart of participants is displayed in Figure 1. Among the 87 asbestos-exposed workers referred to our radiology department, 29 gave their consent and, 27 were retained for analyses. The mean age of volunteers was 63.3±6.5 years old. The mean duration of occupational exposure was 11.9±9.7 years.

Radiation dose

The average DLP was 16±5 mGy.cm for *Veo* and 125±61 mGy.cm for FBP. The corresponding average effective doses were 0.234±0.073 mSv for *Veo* and 1.825±0.876 mSv for FBP. The dose reduction was calculated to be 87.2% ($p<0.001$).

Quality images assessment

For *Veo* acquisition, respiratory artifacts were graded as "negligible" in 24 cases (89%) for reader 1 and 25 cases (93%) for reader 2, "moderate" in 3 cases (11%) for reader 1 and 2 cases (7%) for reader 2, and no "salient" artifact was recorded. For FBP acquisition, respiratory artifacts were graded as "negligible" in 19 cases (70%) for reader 1 and 24 cases (89%) for reader 2, "moderate" in 7 cases (26%) for reader 1 and 3 cases (11%) for reader 2, and as "salient" in 1 case for reader 1 and in 0 cases for reader 2. *Veo* and FBP did not differ in subjective assessment of respiratory artifacts between the two radiologists ($p=0.16$ for reader 1 and $p=0.65$ for reader 2).

Tables 1 and 2 provide results from *subjective* image noise assessed by the two radiologists, average of objective noise data and SNR. The two protocols differed significantly in *objective* image noise. The ultra-low-dose *Veo* acquisition reduced objective image noise from 13 to 23% and increased SNR from 5 to 33% compared with the standard FBP acquisition.

However, *subjective* image noise rated higher by the two readers in axial and coronal planes, with the exception of parenchymal analysis in the coronal plane for the reader 1 (Table 1).

Pleural plaques

A total of 297 pleural plaques (Figure 2) were observed in 20 participants (74%). Detection of plaque did not differ between *Veo* (259; 87%) and FBP (287; 97%) (p=0.10). The agreement for pleural plaques depiction was 84% with a kappa of 0.05. However, when data were examined only for the presence of pleural plaque (yes or no) in patients, agreement increased to 96% ($\kappa = 0.91$).[28 29] Moreover agreement for size measurement (Lin coefficient) was 0.83 ($p<0.001$) and k coefficient for calcification detection was 0.86.

For one participant, despite a *Veo* acquisition considered normal, FBP acquisition was positive for one isolated plaque.

Simultaneous analysis of *Veo* and FBP acquisitions led us to observe that *Veo* acquisition was responsible for 3 false positives corresponding to intercostal fat or muscles, with 8 false negatives (2.7%).

Pleural thickening

Diffuse pleural thickening (Figure 2) was present in four patients (14.8%). The detection rate for each technique was 100% with a kappa of 1. No pleural effusion was found.

Parenchymal abnormalities

Parenchymal changes were found in 15 participants (55.6%), including subpleural dots, curvilinear subpleural lines, ground glass opacities, septal lines and reticulations. No honeycombing was found. Table 3 summarizes the prevalence (P), inter-rater agreement (τ) and kappa κ between *Veo* and FBP acquisition, and the sensitivity, specificity, predictive positive value and predictive negative value of *Veo* acquisition for each interstitial abnormality.

Pulmonary nodules

Pulmonary nodules (Figure 2) were found in all patients, with a total of 167 nodules. All the nodules detected were smaller than 10 mm. No non-solid or part-solid nodules were observed. Among the 167 recorded nodules, the detection rate did not differ (p = 0.98) between *Veo* (134/167) and standard FBP (133/167), with the same 80% detection rate. The agreement between the two techniques for nodules depiction was 60% (κ = 0.25). Simultaneous analysis of *Veo* and FBP acquisitions led us to observe that *Veo* acquisition was responsible for seven false positives (4%) and four false negatives (2.7%).

Inter-observer agreement

No difference was observed for the inter-observer agreement (kappa) between the two techniques. Inter-observer agreement was low for pleural plaques detection (0.09 for FBP and 0.10 for *Veo*) and fair for nodule detection (0.34 for FBP and 0.34 for *Veo*). The inter-reader agreements for parenchymal interstitial abnormalities and parenchymal diffuse pleural thickening were not evaluated due to their low prevalence.

DISCUSSION

We compared for the first time low-dose CT using *Veo* reconstruction and the gold standard CT using FBP reconstruction to depict asbestos-related abnormalities and pulmonary nodules depiction. The major finding was that *Veo* compared favorably with FBP acquisitions in detecting pleural plaques, diffuse pleural thickening and pulmonary nodules. However, interstitial parenchymal abnormalities were depicted less frequently in *Veo* than FBP acquisitions. Nevertheless, *Veo* delivered 87% less radiation than FBP.

Quality of images

The assessment of image quality showed discordant results. Despite low scanning parameters, the iterative reconstruction method of *Veo* significantly reduced the level of objective noise, but subjective noise parameters increased in comparison with FBP. This discordance may be explained by the novel appearance of *Veo* images requiring adaptation time for the radiologists. Our results are in line with previous results showing a relative noise reduction of 25% obtained from *Veo* (100 kV, 10 mAs) compared with FBP protocol (100 kV, 50-300 mAs).[30]

Pleural plaques

Pleural plaques corresponding to parietal pleura fibrosis are indicators of asbestos-exposure [7] with a prevalence as high as 60% in previously exposed workers [10 31] and 74% in the current study with highly exposed workers. In France, the detection of pleural plaques results in financial compensation for workers and early retirement. Consequently, pleural plaques are accepted only when results are unequivocal. Atypical plaques will only be considered when they occur bilateraly or in multiple sites, and with typical localization. Due to the three cases

of false positive and 8 cases of false negative, the low dose CT with *Veo* reconstruction cannot be used for the first examination, but its use seems possible for patients' follow-up.

Diffuse pleural thickening detection

Our results indicated that a low dose scanner with *Veo* reconstruction was comparable with the FBP gold standard for diffuse pleural thickening detection. The prevalence of thickening was rare thus, we could not obtain statistical significance. However, thickening remains of major importance because diagnosis results not only in compensation, but guarantees a life-long pension. Considering the importance usually noted about these lesions, a *Veo* acquisition should be sufficient in clinical practice.

Parenchymal abnormalities

Reader sensitivity with *Veo* images was poor for interstitial parenchymal abnormalities. No case of true asbestosis was recorded, but 15 patients had non-specific interstitial abnormalities. However, the detection of interstitial abnormalities may be limited by several factors. First, the study was built for asbestos-related diseases. Recording specifications lacked the details required to comprehensively describe the presence of interstitial abnormalities. Therefore, without systematic records, interstitial abnormalities were likely underestimated. Second, *Veo* was always performed after FBP resulting in an increase of gravity-dependent attenuation in the posterior region which may have masked interstitial abnormalities. Third, the acquisitions were performed in the supine position and acquisitions in the prone position were not always performed when necessary. Subsequently, the posterior region was not analyzed with confidence. Thus, interstitials abnormalities were underestimated in our study.

Asbestosis refers to interstitial fibrosis caused by the deposition of asbestos fibers in the lung. Its prevalence is estimated to be about 5% in asbestos exposed workers.[32] Asbestosis remains difficult to diagnose, particularly in early stages. However, a significant dose-effect relationship exists between the cumulative exposure to asbestos and asbestosis.[33] Asbestosis is usually associated with dyspnea, basilar rales, and changes in pulmonary function with restrictive or mixed restrictive-obstructive patterns, and carbon monoxide diffusion abnormalities. Pulmonary asbestosis was previously diagnosed in 51 of 706 (7%) of asbestos-exposed workers.[34] In a previous study, 51 of the 706 (7%) of asbestos-exposed workers were diagnosed with pulmonary asbestosis. In this study, only 2% of the workers with less than 25 years of cumulative exposure to asbestos were diagnosed with asbestosis using high resolution CT screening.[34] Therefore, CT screening for asbestosis does not seem warranted in workers with low occupational exposure.

Pulmonary nodules

In our study, all individuals had at least one pulmonary nodule. FBP and *Veo* shared the same detection rate of 80%. However, *Veo* reconstruction is not advised for initial nodules screening due to the 7 false positives and 4 false negatives from the 167 nodules. According to the Fleischner Society guidelines [35], nodule detection on CT requires specific management. In agreement with our recommendations for pleural plaques detection, *Veo* should be used only for patients' follow-up after a first detection of pulmonary nodules using gold standard CT.

Limitations

The sample size could be perceived as a limitation. Limited sample size exacerbated the need for rapid adaptation time by the radiologists with relatively novel images. However,

statistically, the high prevalence of pleural plaques (297, observed in 74% of participants) and pulmonary nodules (167) permitted a robust statistical analysis. Considering these results ($\kappa = 0.91$), power seemed satisfactory (80%) to reject the null hypothesis "H0: $\kappa = 0.4$" vs. "H1: $\kappa \neq 0.91$" with 27 patients. In contrast, parenchymal interstitial abnormalities were rare, precluding sound statistical analyses. Parenchymal interstitial abnormalities suffered from majors limitations due to CT positioning of patients. A further study dedicated to parenchymal interstitial abnormalities should be conducted. Clinically, a current limitation of iterative reconstruction is a long computing time.

CONCLUSION

A low dose computed tomography with *Veo* reconstruction substantially reduces radiation. Despite an unusual appearance, *Veo* image quality was generally accurate in its diagnosis. Specifically, *Veo* compared favorably with the gold standard filtered back projection acquisitions in detecting pleural plaques, diffuse pleural thickening and pulmonary nodules. However, due to a few false positives and false negatives, *Veo* may be best used for follow-up of patients after initial screening with filtered back projection.

Funding The study was funded by the University Hospital CHU G. Montpied, 58 rue Montalembert 63000 Clermont-Ferrand, France. The funders had no role in study design, data collection and analysis, decision to publish, or preparation of the manuscript.

Contributors MT has participated as a MD student and principal investigator. MT, FD, AC and JLM obtained research funding and generated the intellectual development of the study. MT and FD obtained the ethics approval. FD and AC recruited all participants. RB and AR

completed the double blind analyses of Veo and FBP images. MT and BP made data analysis. MT drafted the manuscript. FD and GN revised the manuscript. All authors read and approved the final manuscript.

Acknowledgments Our thanks to the "CAPER des Combrailles" (Association of the asbestos-exposed workers), which helped us recruit the asbestos-exposed workers.

Competing interests None.

Ethics approval Approval was given by the regional ethics committee (ClinicalTrials.gov number: NCT01955018).

Data sharing statement Original data from this study are available by contacting the corresponding author via email.

REFERENCES

1 Stayner L, Welch LS, Lemen R. The worldwide pandemic of asbestos-related diseases. *Annual Review of Public Health* 2013;34:205-16.

2 Oksa P, Pukkala E, Karjalainen A, Ojajarvi A, Huuskonen MS. Cancer incidence and mortality among Finnish asbestos sprayers and in asbestosis and silicosis patients. *American Journal of Industrial Medicine* 1997;31:693-8.

3 Koskinen K, Pukkala E, Martikainen R, Reijula K, Karjalainen A. Different measures of asbestos exposure in estimating risk of lung cancer and mesothelioma among

construction workers. *Journal of Occupational and Environmental Medicine* 2002;44:1190-6.

4 Clin B, Morlais F, Guittet L et al. Performance of chest radiograph and CT scan for lung cancer screening in asbestos-exposed workers. *Occupational and Environmental Medicine* 2009;66:529-34.

5 Fasola G, Belvedere O, Aita M et al. Low-dose computed tomography screening for lung cancer and pleural mesothelioma in an asbestos-exposed population: baseline results of a prospective, nonrandomized feasibility trial--an Alpe-adria Thoracic Oncology Multidisciplinary Group Study (ATOM 002). *The Oncologist* 2007;12:1215-24.

6 Vierikko T, Jarvenpaa R, Autti T et al. Chest CT screening of asbestos-exposed workers: lung lesions and incidental findings. *European Respiratory Journal* 2007;29:78-84.

7 American Thoracic Society. Diagnosis and initial management of nonmalignant diseases related to asbestos. *American Journal of Respiratory and Critical Care Medicine* 2004;170:691-715.

8 Akira M, Yamamoto S, Yokoyama K et al. Asbestosis: high-resolution CT-pathologic correlation. *Radiology* 1990;176:389-94.

9 Akira M, Yokoyama K, Yamamoto S et al. Early asbestosis: evaluation with high-resolution CT. *Radiology* 1991;178:409-16.

10 Neri S, Antonelli A, Falaschi F, Boraschi P, Baschieri L. Findings from high resolution computed tomography of the lung and pleura of symptom free workers exposed to amosite who had normal chest radiographs and pulmonary function tests. *Occupational and Environmental Medicine* 1994;51:239-43.

11 Mettler FA, Jr., Thomadsen BR, Bhargavan M et al. Medical radiation exposure in the U.S. in 2006: preliminary results. *Health Physics* 2008;95:502-7.

12 Samara ET, Aroua A, Bochud FO et al. Exposure of the Swiss population by medical x-rays: 2008 review. *Health Physics* 2012;102:263-70.

13 Shrimpton PC, Hillier MC, Lewis MA, Dunn M. National survey of doses from CT in the UK: 2003. *British Journal of Radiology* 2006;79:968-80.

14 Brenner DJ, Hall EJ. Computed tomography--an increasing source of radiation exposure. *New England Journal of Medicine* 2007;357:2277-84.

15 Marin D, Nelson RC, Schindera ST et al. Low-tube-voltage, high-tube-current multidetector abdominal CT: improved image quality and decreased radiation dose with adaptive statistical iterative reconstruction algorithm--initial clinical experience. *Radiology* 2010;254:145-53.

16 Pontana F, Duhamel A, Pagniez J et al. Chest computed tomography using iterative reconstruction vs filtered back projection (Part 2): image quality of low-dose CT examinations in 80 patients. *European Radiology* 2011;21:636-43.

17 Pontana F, Pagniez J, Flohr T et al. Chest computed tomography using iterative reconstruction vs filtered back projection (Part 1): Evaluation of image noise reduction in 32 patients. *European Radiology* 2011;21:627-35.

18 Ren Q, Dewan SK, Li M et al. Comparison of adaptive statistical iterative and filtered back projection reconstruction techniques in brain CT. *European Journal of Radiology* 2012;81:2597-601.

19 Silva AC, Lawder HJ, Hara A, Kujak J, Pavlicek W. Innovations in CT dose reduction strategy: application of the adaptive statistical iterative reconstruction algorithm. *AJR. American Journal of Roentgenology* 2010;194:191-9.

20 Singh S, Kalra MK, Gilman MD et al. Adaptive statistical iterative reconstruction technique for radiation dose reduction in chest CT: a pilot study. *Radiology* 2011;259:565-73.

21 Mieville FA, Gudinchet F, Brunelle F, Bochud FO, Verdun FR. Iterative reconstruction methods in two different MDCT scanners: physical metrics and 4-alternative forced-choice detectability experiments--a phantom approach. *Phys Med* 2013;29:99-110.

22 Gevenois PA, de Maertelaer V, Madani A, Winant C, Sergent G, De Vuyst P. Asbestosis, pleural plaques and diffuse pleural thickening: three distinct benign responses to asbestos exposure. *European Respiratory Journal* 1998;11:1021-7.

23 Roach HD, Davies GJ, Attanoos R, Crane M, Adams H, Phillips S. Asbestos: when the dust settles an imaging review of asbestos-related disease. *Radiographics* 2002;22 Spec No:S167-84.

24 Jankowski A, Martinelli T, Timsit JF et al. Pulmonary nodule detection on MDCT images: evaluation of diagnostic performance using thin axial images, maximum intensity projections, and computer-assisted detection. *European Radiology* 2007;17:3148-56.

25 Deak PD, Smal Y, Kalender WA. Multisection CT protocols: sex- and age-specific conversion factors used to determine effective dose from dose-length product. *Radiology* 2010;257:158-66.

26 Szucs-Farkas Z, Strautz T, Patak MA, Kurmann L, Vock P, Schindera ST. Is body weight the most appropriate criterion to select patients eligible for low-dose pulmonary CT angiography? Analysis of objective and subjective image quality at 80 kVp in 100 patients. *European Radiology* 2009;19:1914-22.

27 Nam JM. Testing the Intraclass Version of Kappa Coeffcient of Agreement with Binary Scale and Sample Size Determination. *Biometrical Journal* 2002;44:558-570.

28 Cicchetti DV, Feinstein AR. High agreement but low kappa: II. Resolving the paradoxes. *Journal of Clinical Epidemiology* 1990;43:551-8.

29 Feinstein AR, Cicchetti DV. High agreement but low kappa: I. The problems of two paradoxes. *Journal of Clinical Epidemiology* 1990;43:543-9.

30 Mieville FA, Berteloot L, Grandjean A et al. Model-based iterative reconstruction in pediatric chest CT: assessment of image quality in a prospective study of children with cystic fibrosis. *Pediatric Radiology* 2013;43:558-67.

31 Friedman AC, Fiel SB, Fisher MS, Radecki PD, Lev-Toaff AS, Caroline DF. Asbestos-related pleural disease and asbestosis: a comparison of CT and chest radiography. *AJR. American Journal of Roentgenology* 1988;150:269-75.

32 Ross RM. The clinical diagnosis of asbestosis in this century requires more than a chest radiograph. *Chest* 2003;124:1120-8.

33 Green FH, Harley R, Vallyathan V et al. Exposure and mineralogical correlates of pulmonary fibrosis in chrysotile asbestos workers. *Occupational and Environmental Medicine* 1997;54:549-59.

34 Paris C, Benichou J, Raffaelli C et al. Factors associated with early-stage pulmonary fibrosis as determined by high-resolution computed tomography among persons occupationally exposed to asbestos. *Scandinavian Journal of Work, Environment and Health* 2004;30:206-14.

35 MacMahon H, Austin JH, Gamsu G et al. Guidelines for management of small pulmonary nodules detected on CT scans: a statement from the Fleischner Society. *Radiology* 2005;237:395-400.

Table 1 Subjective noise assessment

	Axial mediastinum		Axial parenchyma		Coronal mediastinum		Coronal parenchyma	
	Véo	FBP	Véo	FBP	Véo	FBP	Véo	FBP
Reader 1								
Minimal, no(%)	2 (7)	22 (82)	6 (21)	25 (93)	19 (68)	25 (93)	22 (79)	26 (96)
Moderate, no(%)	19 (68)	5 (18)	18 (64)	2 (7)	8 (32)	2 (7)	5 (21)	1 (4)
Important, no(%)	6 (25)	0	3 (14)	0	0	0	0	0
P value	<0.001		<0.001		0.03		0.10	
Reader 2								
Minimal, no(%)	2 (7)	17 (64)	4 (14)	26 (96)	8 (29)	19 (68)	19 (68)	26 (96)
Moderate, no(%)	14 (50)	10 (36)	18 (64)	1 (4)	17 (61)	7 (29)	8 (32)	1 (4)
Important, no(%)	11 (43)	0	5 (21)	0	2 (11)	1 (4)	0	0
P value	<0.001		<0.001		0.02		<0.01	

Table 2 Objective noise, mean values of SD and SNR measurements

	Objective noise				Signal to Noise Ratio			
	Veo (UH)	FBP (UH)	P value	Decrease (%)	*Veo*	FBP	P value	Increase (%)
Trachea								
Axial	20.12 (3.62)	26.11 (9.34)	<0.01	23%	47.50 (7.84)	42.48 (10.86)	0.04	12
Coronal	21.09 (3.36)	24.37 (7.12)	0.02	13%	45.7 (7.31)	43.39 (9.65)	0.24	5
Descending aorta								
Axial	20.12 (3.19)	25.12 (5.41)	<0.001	20%	1.67 (0.55)	1.28 (0.32)	<0.001	33
Coronal	19.78 (3.32)	24.47 (4.51)	<0.001	19%	1.64 (0.55)	1.34 (0.32)	<0.01	22
Lung								
Axial	25.82 (5.10)	32.83(14.37)	0.02	21%	34.13 (6.62)	31.57 (10.49)	0.25	8
Coronal	27.15 (6.14)	34.26 (10.45)	<0.001	21%	32.25 (7.30)	28.47 (6.94)	0.03	13

Table 3 Low dose CT scan with *Veo* reconstruction, accurately for interstitials abnormalities

	P	τ	κ	Se (IC95%)	Sp (IC95%)	PPV (IC95%)	PNV (IC95%)
Total	**55.6%**	**70.37%**	**0.44**	**46.7%** (21.3-73.4)	**100%** (73.5-100)	**100%** (59-100)	**60%** 36.1-80.9)
Subpleural dots and branching opacities	**33.3%**	**74%**	**0.34**	**33.3%** (7.5-70.1)	**94.4%** (72.7-99.9)	**75%** (19.4-99.4)	**73.9%** (51.6-89.8)
Curvilinear subpleural lines	**8%**	**0**	**0**	**0**	**0**	**0**	**0**
Areas of ground glass opacities	**25.9%**	**77.8%**	**0.2**	**14.3%** (0.4-57.9)	**100%** (83.2-100)	**100%** (2.5-100)	**76.9%** (56.4-91)
Honeycombing	**0**						
Réticulations	**18.5%**	**92.6%**	**0.71**	**60%** (14.7-94.7)	**100%** (84.6-100)	**100%** (29.2-100)	**91.7%** (73-99)
Septal lines	**14.8%**	**85.2%**	**0.26**	**25%** (0.6-80.6)	**95.7%** (78.1-99.9)	**50%** (1.3-98.7)	**88%** (68.8-97.5)

P: prevalence, τ: Agreement with standard CT scan, κ: kappa coefficient, Se: sensitivity, Sp: specificity, PPV: Positive Predictive Value, PVN: Predictive Negative value.

Figure 1 Flow-chart of participants.

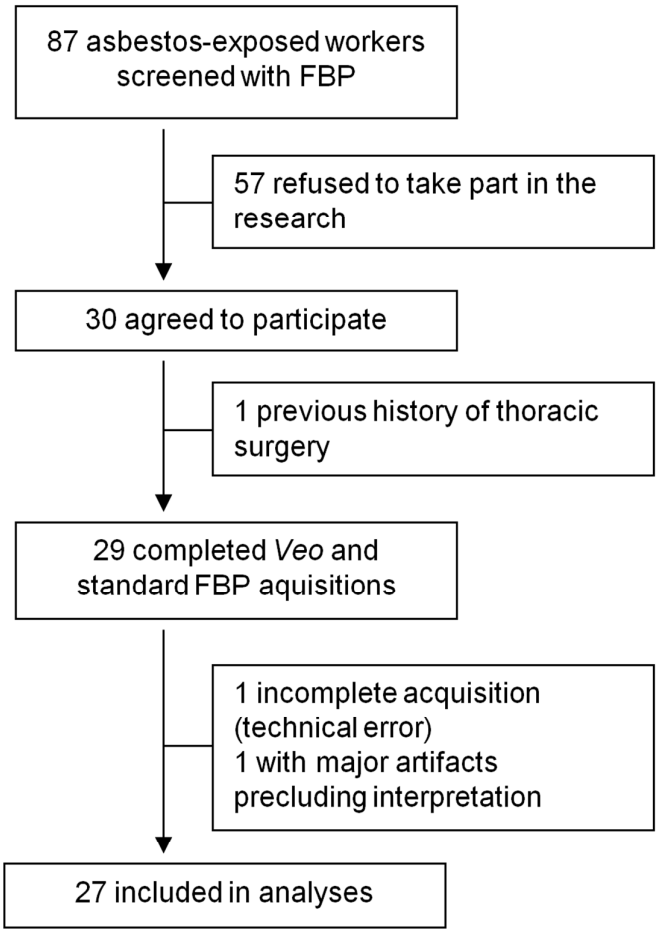

Figure 2 Typical pleural plaques (1. white arrows), diffuse pleural thickening (2. white arrows) and parenchymal band (2. black arrows), and pulmonary nodule (3. white arrows) in axial plane and an example of normal images in axial plane (4). All Veo and FBP images are captured at the same anatomic level, with 100 kV and 20 mAs per section for *Veo* and 120 kV, 60 mAs for FBP.

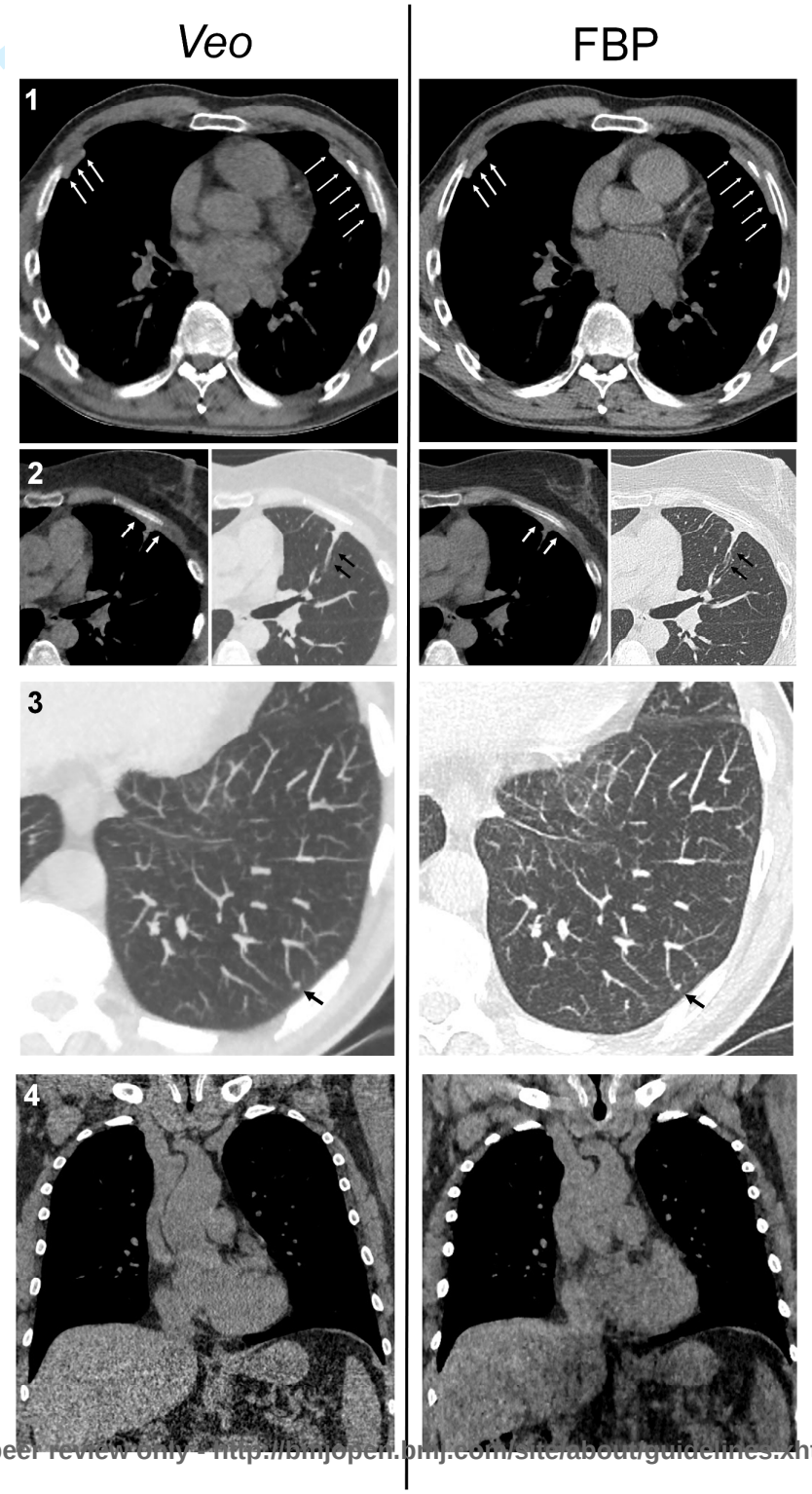

STARD checklist for reporting of studies of diagnostic accuracy

(version January 2003)

Section and Topic	Item #		On page #
TITLE/ABSTRACT/ KEYWORDS	1	Identify the article as a study of diagnostic accuracy (recommend MeSH heading 'sensitivity and specificity').	1
INTRODUCTION	2	State the research questions or study aims, such as estimating diagnostic accuracy or comparing accuracy between tests or across participant groups.	3
METHODS			
Participants	3	The study population: The inclusion and exclusion criteria, setting and locations where data were collected.	4
	4	Participant recruitment: Was recruitment based on presenting symptoms, results from previous tests, or the fact that the participants had received the index tests or the reference standard?	4
	5	Participant sampling: Was the study population a consecutive series of participants defined by the selection criteria in item 3 and 4? If not, specify how participants were further selected.	Yes (4)
	6	Data collection: Was data collection planned before the index test and reference standard were performed (prospective study) or after (retrospective study)?	Prospective: see page 4 and stats page 7
Test methods	7	The reference standard and its rationale.	7
	8	Technical specifications of material and methods involved including how and when measurements were taken, and/or cite references for index tests and reference standard.	4 to 6
	9	Definition of and rationale for the units, cut-offs and/or categories of the results of the index tests and the reference standard.	4 to 6
	10	The number, training and expertise of the persons executing and reading the index tests and the reference standard.	Page 5: Interpretation of CT Images
	11	Whether or not the readers of the index tests and reference standard were blind (masked) to the results of the other test and describe any other clinical information available to the readers.	Page 5: Interpretation of CT Images
Statistical methods	12	Methods for calculating or comparing measures of diagnostic accuracy, and the statistical methods used to quantify uncertainty (e.g. 95% confidence intervals).	7
	13	Methods for calculating test reproducibility, if done.	NA
RESULTS			
Participants	14	When study was performed, including beginning and end dates of recruitment.	4: between September 2012, and April 2013
	15	Clinical and demographic characteristics of the study population (at least information on age, gender, spectrum of presenting symptoms).	8
	16	The number of participants satisfying the criteria for inclusion who did or did not undergo the index tests and/or the reference standard; describe why participants failed to undergo either test (a flow diagram is strongly recommended).	8 and figure 3 flow chart
Test results	17	Time-interval between the index tests and the reference standard, and any treatment administered in between.	Simultaneously: see CT protocol pages 6-7
	18	Distribution of severity of disease (define criteria) in those with the target condition; other diagnoses in participants without the target condition.	9-10 if applicable
	19	A cross tabulation of the results of the index tests (including indeterminate and missing results) by the results of the reference standard; for continuous results, the distribution of the test results by the results of the reference standard.	See tables
	20	Any adverse events from performing the index tests or the reference standard.	Impossible to have an adverse event with Veo
Estimates	21	Estimates of diagnostic accuracy and measures of statistical uncertainty (e.g. 95% confidence intervals).	See limitations p14 and p9-10

	22	How indeterminate results, missing data and outliers of the index tests were handled.	Excluded: page 8 and flow chart figure 3
	23	Estimates of variability of diagnostic accuracy between subgroups of participants, readers or centers, if done.	NA
	24	Estimates of test reproducibility, if done.	NA
DISCUSSION	25	Discuss the clinical applicability of the study findings.	Page 13

BMJ Open

Comparison of the ultra-low-dose Veo algorithm with the gold standard filtered back projection for detecting pulmonary asbestos-related conditions: a clinical observational study

Journal:	*BMJ Open*
Manuscript ID:	bmjopen-2014-004980.R1
Article Type:	Research
Date Submitted by the Author:	30-Apr-2014
Complete List of Authors:	Tekath, Marielle; University Hospital CHU Clermont-Ferrand, Dutheil, Frederic; CHU G Montpied, Occupational Medicine Bellini, Romain; University Hospital CHU Clermont-Ferrand, Roche, Antoine; University Hospital CHU Clermont-Ferrand, Pereira, Bruno; University Hospital CHU Clermont-Ferrand, Naughton, Geraldine; Australian Catholic University, School of Exercise Science Chamoux, Alain; CHU G. Montpied, Occupational Medicine Michel, Jean-Luc; University Hospital CHU Clermont-Ferrand,
Primary Subject Heading:	Occupational and environmental medicine
Secondary Subject Heading:	Radiology and imaging, Public health
Keywords:	OCCUPATIONAL & INDUSTRIAL MEDICINE, Computed tomography < RADIOLOGY & IMAGING, PUBLIC HEALTH

Comparison of the ultra-low-dose *Veo* algorithm with the gold standard filtered back projection for detecting pulmonary asbestos-related conditions: a clinical observational study

Marielle Tekath[1], Frédéric Dutheil[2,3,4,5], Romain Bellini[6], Antoine Roche[1], Bruno Pereira[7], Geraldine Naughton[3,*], Alain Chamoux[2], Jean-Luc Michel[1]

[1] Department of Radiology, University Hospital CHU G. Montpied, Clermont-Ferrand, France

[2] Occupational Medicine, University Hospital CHU G. Montpied, Clermont-Ferrand, France

[3] School of Exercise Science, Australian Catholic University, Locked Bag 4115, Fitzroy MDC, VIC 3065, Australia

[4] Laboratory of Metabolic Adaptations to Exercise in Physiological and Pathological conditions EA3533, Blaise Pascal University, Clermont-Ferrand, France

[5] INRA, UMR 1019, UNH, CRNH Auvergne, Clermont-Ferrand, France

[6] Department of Radiology, Centre Jean Perrin, University Hospital CHU Clermont-Ferrand, France

[7] Department of Medical Statistics, University Hospital CHU G. Montpied, Clermont-Ferrand, France

*** Correspondance to**: Geraldine Naughton; Geraldine.Naughton@acu.edu.au

Running title: *Veo* in asbestos-related conditions

Words count for introduction methods results discussion and conclusion: 2946

Number of tables: 3

Number of figures: 2

Words count for abstract: 249

ABSTRACT

Objectives: Radiation delivered during computed tomography is a major concern, especially for individuals undergoing repeated screening. We aimed to compare a new ultra-low dose algorithm called *Veo* with the gold standard filtered back projection (FBP) for detecting pulmonary asbestos-related conditions.

Setting: University Hospital CHU G. Montpied, Clermont-Ferrand, France

Participants: Asbestos-exposed workers were recruited following referral to screening for asbestos-related conditions. Two acquisitions were performed on a 64-slice computed tomography: the gold standard FBP followed by *Veo* reconstruction.

Outcome measures: Two radiologists independently assessed asbestos-related abnormalities, pulmonary nodules, radiation doses, and image quality (noise).

Results: We included 27 asbestos-exposed workers (63.3±6.5 years with 11.9±9.7 years of asbestos-exposure). We observed 297 pleural plaques in 20 participants (74%). All patients (100%) had pulmonary nodules, totaling 167 nodules. Detection rates did not differ for pleural plaques (*Veo* 87% vs. FBP 97%, NS), pleural thickening (100% for both) and pulmonary nodules (80% for both). Interstitial abnormalities were depicted less frequently with *Veo* than FBP. False negative and false positive did not exceed 2.7%. Compared with FBP, *Veo* decreased the radiation dose up to 87% (*Veo* 0.23±0.07 vs. FBP 1.83±0.88 mSv, $p<0.001$). The objective image noise also decreased with *Veo* as much as 23% and signal to noise ratio increased up to 33%.

Conclusion: A low dose computed tomography with *Veo* reconstruction substantially reduced radiation. *Veo* compared favorably with FBP in detecting pleural plaques, pleural thickening and pulmonary nodules. These results should be confirmed on a larger sample size before the use of *Veo* in clinical routine practice in asbestos-related conditions, especially regarding the low prevalence of interstitial abnormalities in this study (ClinicalTrials.gov number: NCT01955018).

Keywords computed tomography, radiation, screening, asbestos, workers, cancer

Strengths and limitations of this study

- Radiation delivered during computed tomography is a major concern, especially for individuals undergoing repeated screening, such as asbestos-exposed workers.
- We provides the first comparison of a new ultra-low dose algorithm called *Veo* ("I see" in Spanish) with the gold standard filtered back projection (FBP) in detecting pulmonary conditions in asbestos-exposed workers.
- *Veo* substantially reduces radiation doses, with 87% less radiation delivered than FBP.
- *Veo* compared favorably with FBP acquisitions in detecting pleural plaques, diffuse pleural thickening and pulmonary nodules; the high prevalence of pleural plaques (297, observed in 74% of participants) and pulmonary nodules (167) permitted a robust statistical analysis.
- However, these results should be confirmed on a larger sample size before the use of *Veo* in clinical routine practice in asbestos-related conditions, especially regarding the low prevalence of interstitial abnormalities.

INTRODUCTION

Asbestos fibers were intensively used throughout the 20th century, and remain prevalent in developing countries.[1] However, asbestos exposure induces a variety of benign and malignant pleural and lung diseases.[2 3] Due to a long latency period between exposure and disease presentation, asbestos-related diseases remain a substantial public health problem.[1] The most common asbestos-induced neoplasm is lung cancer.[2 3] Chest computed tomography (CT) screening has been successfully used in the early detection of lung cancer in asbestos-exposed workers.[4-6] Moreover, thin-section CT is more sensitive than a chest x-ray for detecting early asbestos-related conditions.[7-10] Nevertheless, the use of CT has two main disadvantages: high radiation doses and depiction of incidental abnormalities such as pulmonary nodules in asymptomatic patients. Incidental abnormalities increase the frequency of follow-up by CT and may also psychologically impact on patients. Medical exposure from x-rays represents the major source of man-made irradiation with a large contribution from CT.[11-13] Increased exposure to radiation underpins the consequences of cancer induction.[14] However, reducing CT doses increases image noise from the filtered back projection (FBP) reconstruction. Strategies to reduce radiation exposure include the use of iterative reconstruction algorithms such as "iDose", "100% ASIR" and "IRIS".[15-20] The new algorithm called *Veo*™ (General Electric Healthcare, Milwaukee, MI, USA) decreases the image noise up to 70% compared with the gold standard FBP model, whereas the "100% ASIR" algorithm is only capable of reducing image noise up to 47%.[21] Moreover, *Veo* ("I see" in Spanish) improves spatial resolution with excellent detection of low and high contrast objects from a CT Dose Index ($CTDI_{vol}$) equal to 0.3 mGy.

Thus, the objective of the present study was to compare *Veo* with the gold standard FBP for detecting pulmonary asbestos-related conditions among workers previously exposed to asbestos. Comparisons included radiation delivered and image quality.

METHODS

Patients

Our clinical observational study received approval from the ethical committee of the University Hospital of Clermont-Ferrand (ClinicalTrials.gov number: NCT01955018). Written informed consent was obtained from all participants for the supplementary acquisition of *Veo* images in addition to their clinically indicated chest CT. Asbestos-exposed workers were recruited following referral to our radiology department for the evaluation of asbestos-related disease between September 2012, and April 2013. Inclusion criteria were being an asbestos-exposed workers, having a chest CT referral from the occupational medicine department, no history of cancer or thoracic surgery, and the absence of other known interstitial pathology.

CT protocol

CT examinations were performed with a 64-slice CT system (Discovery CT 750HD; GE Healthcare, Milwaukee, WI) and consisted of two successive acquisitions. Each examination, the normal-dose (FBP acquisition) and ultra-low-dose (*Veo* acquisition) spiral CT, was obtained on the entire thorax, at full inspiration with the participant in the supine position. No intravenous contrast material was administered. In accordance with guidelines, standard acquisition was performed with CT parameters adjusted to the participant's body size, including a tube kilovoltage (kV) of 120 (participants weighing 70 kg or less) and 140 (participants weighing more than 70 kg), with milliamperage (mA) equal to the patient's body weight. The other CT parameters were rotation time 0.5 s and pitch 1.375. Image data were

reconstructed with FBP algorithm. The *Veo* acquisition was performed with constant CT parameters including: a tube voltage of 100 kV, a tube current of 20 mA, pitch of 0.984 and rotation time 0.4 s. Image data were reconstructed with the *Veo* algorithm.

Interpretation of CT Images

Each CT acquisition was viewed independently by two radiologists (2 and 7 years of experience – Drs RB and AR). The low-dose images with *Veo* reconstruction were interpreted before the standard CT and on separate weeks to minimize recall bias. A third simultaneous reading of the *Veo* and FBP acquisitions by the more experienced radiologist (AR) evaluated the concordance of pleuroparenchymal abnormalities between *Veo* and FBP. Because FBP images are benchmark practice, when a lesion was found only on *Veo* images, it was regarded as a false positive.

Pleural and parenchymal abnormalities

According to established criteria,[9 22 23] the following asbestos-related pleural and parenchymal abnormalities were recorded as present or absent. Pleural abnormalities considered were:

- Pleural plaques: pleura thickening with no associated parenchymal abnormality. We recorded for each lesion: localization (side, region: anterolateral, posterolateral, diaphragmatic or mediastinum), thickness, and calcification.

- Diffuse pleural thickening: pleural thickening associated with parenchymal abnormalities such as rounded atelectasis and parenchymal bands.[22]

- Pleural effusion is typically asymptomatic, the fluid may be serous or hemorrhagic.[22]

CT features of asbestosis included: 1) subpleural dots and branching opacities, 2) curvilinear subpleural lines, defined as linear opacity within 1 cm of the pleura and parallel to the inner chest wall, 3) areas of ground glass opacities, 4) septal lines and 5) reticulations defined as

single or branching lines 1-2 cm in length in the subpleural parenchyma, 6) honeycombing, defined as cystic air spaces with well-defined walls less than 1 cm diameter.

Presence of nodules was also recorded. We noted for each abnormality: localization (side, table position) and nature (non-solid, part-solid, solid or calcified). To increase sensitivity, nodules were examined by combining maximum intensity projections and millimetric axial CT images.[24]

Radiation

Comparisons included the dose length product (DLP) in mGy.cm and effective doses in mSv. Computed conversion factor from DLP to effective dose for adult chest is 0.0146 $mSv.mGy^{-1}.cm^{-1}$ [25].

Quality of FBP and *Veo* Images

Respiratory artifacts were graded on a three-point scale (1 = negligible, 2 = moderate, 3 = salient). Images noise was studied in the axial and coronal planes. A similar scale was used for subjective image quality in the mediastinum and parenchyma windows. Objective image noise is the mean of the Standard Deviation of the signal intensity (in Hounsfield's units) measured with circular regions of interest (ROI) on different anatomical levels, 10 mm in diameter.[19] ROIs were drawn within the descending thoracic aorta at the level of the left main bronchus, within the tracheal lumen up to the tracheal bifurcation, and on the lung. The signal to noise ratio (SNR) was also calculated using the equation SNR = signal intensity / objective noise.[26]

Statistical Analysis

Sample size estimation was based on the number of pleural plaques and nodules. Considering the investigative nature of the study design and because the number of pleural plaques and nodules was not known initially, a sample size estimation was not proposed *a priori* even though a concordance coefficient kappa (κ) between 0.40 and 0.90 was expected between filtered back projection images and *Veo* images. Therefore, 30 asbestos-exposed workers were predicted to be necessary to reject the null hypothesis "H0: $\kappa = 0.40$" vs. "H1: $\kappa \neq 0.75$" for a proportion of pleural plaques of 65%, with a statistical power of > 85% and α=5% (two-sided). Finally, the study was conducted to sequentially control the statistical power considering the number of plaques and nodules for each asbestos-exposed worker.[27]

Statistical analysis was performed using Stata software (version 12; Stata-Corp, College Station, Tex., USA). Quantitative variables are expressed as means ± standard deviations (SD). Proportions are expressed as percentage and 95% confidence intervals (CIs). Comparisons in paired situation were realized using paired Student t-test or Wilcoxon test when appropriate for quantitative variables and Stuart-Maxwell test for categorical parameters. Sensitivity, specificity, false positives and false negatives values of *Veo* were calculated and presented with 95% confidence intervals, in comparison with results from FBP acquisitions. Estimates of sensitivity and specificity were obtained by first estimating the sensitivity and specificity for each patient. Sensitivity and specificity were then estimated by averaging the individual specific estimates across patients. The variance of the estimate was the sample variance divided by the number of patients. Generalized estimating equation models with logit link and working independence correlation structure were also used to estimate sensitivity, taking into account the correlation among the multiple pleural plaques and pulmonary nodules for the same patient. The kappa coefficient was used to measure agreement for categorical parameters and Pearson's correlation coefficient and Lin concordance correlation coefficient for quantitative data. The analyses were completed by

using of random-effect models when appropriate to consider within and between participant variability. The tests were two-sided, with a type I error set at α=0.05.

RESULTS

Patients

The flow chart of participants is displayed in Figure 1. Among the 87 asbestos-exposed workers referred to our radiology department, 29 gave their consent and, 27 were retained for analyses. The mean age of volunteers was 63.3±6.5 years old. The mean duration of occupational exposure was 11.9±9.7 years.

Radiation dose

The average DLP was 16±5 mGy.cm for *Veo* and 125±61 mGy.cm for FBP. The corresponding average effective doses were 0.234±0.073 mSv for *Veo* and 1.825±0.876 mSv for FBP. The dose reduction was calculated to be 87.2% ($p<0.001$).

Quality images assessment

For *Veo* acquisition, respiratory artifacts were graded as "negligible" in 24 cases (89%) for reader 1 and 25 cases (93%) for reader 2, "moderate" in 3 cases (11%) for reader 1 and 2 cases (7%) for reader 2, and no "salient" artifact was recorded. For FBP acquisition, respiratory artifacts were graded as "negligible" in 19 cases (70%) for reader 1 and 24 cases (89%) for reader 2, "moderate" in 7 cases (26%) for reader 1 and 3 cases (11%) for reader 2, and as "salient" in 1 case for reader 1 and in 0 cases for reader 2. *Veo* and FBP did not differ

in subjective assessment of respiratory artifacts between the two radiologists (p=0.16 for reader 1 and p=0.65 for reader 2).

Tables 1 and 2 provide results from *subjective* image noise assessed by the two radiologists using, average of objective noise data and SNR. The two protocols differed significantly in *objective* image noise. The ultra-low-dose *Veo* acquisition reduced objective image noise from 13 to 23% and increased SNR from 5 to 33% compared with the standard FBP acquisition.

However, the two readers rated higher *subjective* image noise in axial and coronal planes with *Veo* than FBP, with the exception of parenchymal analysis in the coronal plane for the reader 1 (Table 1).

Pleural plaques

A total of 297 pleural plaques (Figure 2) were observed in 20 participants (74%). Detection of plaques did not differ between *Veo* (259; 87%) and FBP (287; 97%) (p=0.10). Thus, the third simultaneous reading of *Veo* and FBP resulted in the detection of 10 plaques that were not detected during the first reading of FBP images. The agreement for pleural plaques depiction was 84% with a kappa of 0.05. However, when data were examined only for the presence of pleural plaque (yes or no) in patients, agreement increased to 96% ($\kappa = 0.91$).[28 29] Moreover agreement for size measurement (Lin coefficient) was 0.83 ($p<0.001$) and k coefficient for calcification detection was 0.86.

For one participant, despite a *Veo* acquisition considered normal, FBP acquisition was positive for one isolated plaque.

Simultaneous analysis of *Veo* and FBP acquisitions led us to observe that *Veo* acquisition was responsible for 3 false positives corresponding to intercostal fat or muscles, with 8 false negatives (2.7%).

Pleural thickening

Diffuse pleural thickening (Figure 2) was present in four patients (14.8%). The detection rate for each technique was 100% with a kappa of 1. No pleural effusion was found.

Parenchymal abnormalities

Parenchymal changes were found in 15 participants (55.6%), including subpleural dots, curvilinear subpleural lines, ground glass opacities, septal lines and reticulations. No honeycombing was found. Table 3 summarizes the prevalence (P), inter-rater agreement (τ) and kappa κ between *Veo* and FBP acquisition, and the sensitivity, specificity, predictive positive value and predictive negative value of *Veo* acquisition for each interstitial abnormality.

Pulmonary nodules

Pulmonary nodules (Figure 2) were found in all patients, with a total of 167 nodules. All the nodules detected were smaller than 10 mm. No non-solid or part-solid nodules were observed. Among the 167 recorded nodules, the detection rate did not differ ($p = 0.98$) between *Veo* (134/167) and standard FBP (133/167), with the same 80% detection rate. Thus, the third simultaneous reading of *Veo* and FBP resulted in the detection of 34 nodules that were not detected during the first reading of FBP images..The agreement between the two techniques for nodules depiction was 60% ($\kappa = 0.25$). Simultaneous analysis of *Veo* and FBP acquisitions permitted us to observe that *Veo* acquisition was responsible for seven false positives (4%) and four false negatives (2.7%).

Inter-observer agreement

No difference was observed for the inter-observer agreement (kappa) between the two techniques. Inter-observer agreement was low for pleural plaques detection (0.09 for FBP and 0.10 for *Veo*) and fair for nodule detection (0.34 for FBP and 0.34 for *Veo*). The inter-reader agreements for parenchymal interstitial abnormalities and parenchymal diffuse pleural thickening were not evaluated due to their low prevalence.

DISCUSSION

We compared for the first time low-dose CT using *Veo* reconstruction and the gold standard CT using FBP reconstruction to depict asbestos-related abnormalities and pulmonary nodules depiction. The major finding was that *Veo* compared favorably with FBP acquisitions in detecting pleural plaques, diffuse pleural thickening and pulmonary nodules. However, interstitial parenchymal abnormalities were depicted less frequently in *Veo* than FBP acquisitions. Nevertheless, *Veo* delivered 87% less radiation than FBP.

Quality of images

The assessment of image quality showed discordant results. Despite low scanning parameters, the iterative reconstruction method of *Veo* significantly reduced the level of objective noise, but subjective noise parameters increased in comparison with FBP. This discordance may be explained by the novel appearance of *Veo* images requiring adaptation time for the radiologists. Our results are in line with previous results showing a relative noise reduction of 25% obtained from *Veo* (100 kV, 10 mAs) compared with FBP protocol (100 kV, 50-300 mAs).[30]

Pleural plaques

Pleural plaques corresponding to parietal pleura fibrosis are indicators of asbestos-exposure [7] with a prevalence as high as 60% in previously exposed workers [10 31] and 74% in the current study with highly exposed workers. In France, the detection of pleural plaques results in financial compensation for workers and early retirement. Consequently, pleural plaques are accepted only when results are unequivocal. Atypical plaques will only be considered when they occur bilateraly or in multiple sites, and with typical localization. Due to the three cases of false positive and 8 cases of false negative, the low dose CT with *Veo* reconstruction cannot be used for the first examination, but its use seems possible for patients' follow-up.

Diffuse pleural thickening detection

Our results indicated that a low dose scanner with *Veo* reconstruction was comparable with the FBP gold standard for diffuse pleural thickening detection. The prevalence of thickening was rare thus, we could not obtain statistical significance. However, thickening remains of major importance because diagnosis results not only in compensation, but guarantees a life-long pension. Considering the importance usually noted about these lesions, a *Veo* acquisition should be sufficient in clinical practice.

Parenchymal abnormalities

Reader sensitivity with *Veo* images was poor for interstitial parenchymal abnormalities. No case of true asbestosis was recorded, but 15 patients had non-specific interstitial abnormalities. However, the detection of interstitial abnormalities may be limited by several factors. First, the study was built for asbestos-related diseases. Recording specifications lacked the details required to comprehensively describe the presence of interstitial abnormalities. Therefore, without systematic records, interstitial abnormalities were likely

underestimated. Second, *Veo* was always performed after FBP resulting in an increase of gravity-dependent attenuation in the posterior region which may have masked interstitial abnormalities. Third, the acquisitions were performed in the supine position and acquisitions in the prone position were not always performed when necessary. Subsequently, the posterior region was not analyzed with confidence. Thus, interstitials abnormalities were underestimated in our study.

Asbestosis refers to interstitial fibrosis caused by the deposition of asbestos fibers in the lung. Its prevalence is estimated to be about 5% in asbestos exposed workers.[32] Asbestosis remains difficult to diagnose, particularly in early stages. However, a significant dose-effect relationship exists between the cumulative exposure to asbestos and asbestosis.[33] Asbestosis is usually associated with dyspnea, basilar rales, and changes in pulmonary function with restrictive or mixed restrictive-obstructive patterns, and carbon monoxide diffusion abnormalities. Pulmonary asbestosis was previously diagnosed in 51 of 706 (7%) of asbestos-exposed workers.[34] In a previous study, 51 of the 706 (7%) of asbestos-exposed workers were diagnosed with pulmonary asbestosis. In this study, only 2% of the workers with less than 25 years of cumulative exposure to asbestos were diagnosed with asbestosis using high resolution CT screening.[34] Therefore, CT screening for asbestosis does not seem warranted in workers with low occupational exposure.

Pulmonary nodules

In our study, all individuals had at least one pulmonary nodule. FBP and *Veo* shared the same detection rate of 80%. However, *Veo* reconstruction is not advised for initial nodules screening due to the 7 false positives and 4 false negatives from the 167 nodules. According to the Fleischner Society guidelines [35], nodule detection on CT requires specific management. In agreement with our recommendations for pleural plaques detection, *Veo* should be used

only for patients' follow-up after a first detection of pulmonary nodules using gold standard CT.

Comparison of *Veo* with other low-dose algorithms

To date, no studies using other algorithms to reduce radiation exposure have investigated asbestos-related conditions. Thus, because the *Veo* algorithm appears to reduce the more radiation delivered than other low-dose algorithm such as "iDose", "100% ASIR" or "IRIS"[15-20], we chose only to compare *Veo* with the gold standard FBP.

Limitations

The sample size could be perceived as a limitation. Limited sample size exacerbated the need for rapid adaptation time by the radiologists with relatively novel images. However, statistically, the high prevalence of pleural plaques (297, observed in 74% of participants) and pulmonary nodules (167) permitted a robust statistical analysis. Considering these results (κ = 0.91), power seemed satisfactory (80%) to reject the null hypothesis "H0: $\kappa = 0.4$" vs. "H1: $\kappa \neq 0.91$" with 27 patients. In contrast, parenchymal interstitial abnormalities were rare, precluding sound statistical analyses. Parenchymal interstitial abnormalities suffered from majors limitations due to CT positioning of patients. A further study dedicated to parenchymal interstitial abnormalities should be conducted. Clinically, a current limitation of iterative reconstruction is a long computing time.

CONCLUSION

A low dose computed tomography with *Veo* reconstruction substantially reduces radiation. Despite an unusual appearance, *Veo* image quality was generally accurate in its diagnosis. Specifically, *Veo* compared favorably with the gold standard filtered back projection

acquisitions in detecting pleural plaques, diffuse pleural thickening and pulmonary nodules. However, these results should be confirmed on a larger sample size before the use of *Veo* in clinical routine practice in asbestos-related conditions, especially regarding the low prevalence of interstitial abnormalities in this study.

Acknowledgments Our thanks to the "CAPER des Combrailles" (Association of the asbestos-exposed workers), which helped us recruit the asbestos-exposed workers.

Funding The study was funded by the University Hospital CHU G. Montpied, 58 rue Montalembert 63000 Clermont-Ferrand, France. The funders had no role in study design, data collection and analysis, decision to publish, or preparation of the manuscript.

Contributors MT has participated as a MD student and principal investigator. MT, FD, AC and JLM obtained research funding and generated the intellectual development of the study. MT and FD obtained the ethics approval. FD and AC recruited all participants. RB and AR completed the double blind analyses of *Veo* and FBP images. MT and BP made data analysis. MT drafted the manuscript. FD and GN revised the manuscript. All authors read and approved the final manuscript.

Competing interests None.

Ethics approval Approval was given by the regional ethics committee (ClinicalTrials.gov number: NCT01955018).

Data sharing statement Original data (crude data) from this study are available by contacting the corresponding author via email.

Figure legends

Figure 1 Flow-chart of participants.

Figure 2 Typical pleural plaques (1. white arrows), diffuse pleural thickening (2. white arrows) and parenchymal band (2. black arrows), and pulmonary nodule (3. white arrows) in axial plane and an example of normal images in axial plane (4). All *Veo* and FBP images are captured at the same anatomic level, with 100 kV and 20 mAs per section for *Veo* and 120 kV, 60 mAs for FBP.

REFERENCES

1 Stayner L, Welch LS, Lemen R. The worldwide pandemic of asbestos-related diseases. *Annual Review of Public Health* 2013;**34**:205-16.

2 Oksa P, Pukkala E, Karjalainen A, et al. Cancer incidence and mortality among Finnish asbestos sprayers and in asbestosis and silicosis patients. *American Journal of Industrial Medicine* 1997;**31**:693-8.

3 Koskinen K, Pukkala E, Martikainen R, et al. Different measures of asbestos exposure in estimating risk of lung cancer and mesothelioma among construction workers. *Journal of Occupational and Environmental Medicine* 2002;**44**:1190-6.

4 Clin B, Morlais F, Guittet L et al. Performance of chest radiograph and CT scan for lung cancer screening in asbestos-exposed workers. *Occupational and Environmental Medicine* 2009;**66**:529-34.

5 Fasola G, Belvedere O, Aita M et al. Low-dose computed tomography screening for lung cancer and pleural mesothelioma in an asbestos-exposed population: baseline results of a prospective, nonrandomized feasibility trial--an Alpe-adria Thoracic Oncology Multidisciplinary Group Study (ATOM 002). *The Oncologist* 2007;**12**:1215-24.

6 Vierikko T, Jarvenpaa R, Autti T et al. Chest CT screening of asbestos-exposed workers: lung lesions and incidental findings. *European Respiratory Journal* 2007;**29**:78-84.

7 American Thoracic Society. Diagnosis and initial management of nonmalignant diseases related to asbestos. *American Journal of Respiratory and Critical Care Medicine* 2004;**170**:691-715.

8 Akira M, Yamamoto S, Yokoyama K et al. Asbestosis: high-resolution CT-pathologic correlation. *Radiology* 1990;**176**:389-94.

9 Akira M, Yokoyama K, Yamamoto S et al. Early asbestosis: evaluation with high-resolution CT. *Radiology* 1991;**178**:409-16.

10 Neri S, Antonelli A, Falaschi F, et al. Findings from high resolution computed tomography of the lung and pleura of symptom free workers exposed to amosite who had normal chest radiographs and pulmonary function tests. *Occupational and Environmental Medicine* 1994;**51**:239-43.

11 Mettler FA, Jr., Thomadsen BR, Bhargavan M et al. Medical radiation exposure in the U.S. in 2006: preliminary results. *Health Physics* 2008;**95**:502-7.

12 Samara ET, Aroua A, Bochud FO et al. Exposure of the Swiss population by medical x-rays: 2008 review. *Health Physics* 2012;**102**:263-70.

13 Shrimpton PC, Hillier MC, Lewis MA, et al. National survey of doses from CT in the UK: 2003. *British Journal of Radiology* 2006;**79**:968-80.

14 Brenner DJ, Hall EJ. Computed tomography--an increasing source of radiation exposure. *New England Journal of Medicine* 2007;**357**:2277-84.

15 Marin D, Nelson RC, Schindera ST et al. Low-tube-voltage, high-tube-current multidetector abdominal CT: improved image quality and decreased radiation dose with adaptive statistical iterative reconstruction algorithm--initial clinical experience. *Radiology* 2010;**254**:145-53.

16 Pontana F, Duhamel A, Pagniez J et al. Chest computed tomography using iterative reconstruction vs filtered back projection (Part 2): image quality of low-dose CT examinations in 80 patients. *European Radiology* 2011;**21**:636-43.

17 Pontana F, Pagniez J, Flohr T et al. Chest computed tomography using iterative reconstruction vs filtered back projection (Part 1): Evaluation of image noise reduction in 32 patients. *European Radiology* 2011;**21**:627-35.

18 Ren Q, Dewan SK, Li M et al. Comparison of adaptive statistical iterative and filtered back projection reconstruction techniques in brain CT. *European Journal of Radiology* 2012;**81**:2597-601.

19 Silva AC, Lawder HJ, Hara A, et al. Innovations in CT dose reduction strategy: application of the adaptive statistical iterative reconstruction algorithm. *AJR. American Journal of Roentgenology* 2010;**194**:191-9.

20 Singh S, Kalra MK, Gilman MD et al. Adaptive statistical iterative reconstruction technique for radiation dose reduction in chest CT: a pilot study. *Radiology* 2011;**259**:565-73.

21 Mieville FA, Gudinchet F, Brunelle F, et al. Iterative reconstruction methods in two different MDCT scanners: physical metrics and 4-alternative forced-choice detectability experiments--a phantom approach. *Phys Med* 2013;**29**:99-110.

22 Gevenois PA, de Maertelaer V, Madani A, et al. Asbestosis, pleural plaques and diffuse pleural thickening: three distinct benign responses to asbestos exposure. *European Respiratory Journal* 1998;**11**:1021-7.

23 Roach HD, Davies GJ, Attanoos R, et al. Asbestos: when the dust settles an imaging review of asbestos-related disease. *Radiographics* 2002;**22 Spec No**:S167-84.

24 Jankowski A, Martinelli T, Timsit JF et al. Pulmonary nodule detection on MDCT images: evaluation of diagnostic performance using thin axial images, maximum intensity projections, and computer-assisted detection. *European Radiology* 2007;**17**:3148-56.

25 Deak PD, Smal Y, Kalender WA. Multisection CT protocols: sex- and age-specific conversion factors used to determine effective dose from dose-length product. *Radiology* 2010;**257**:158-66.

26 Szucs-Farkas Z, Strautz T, Patak MA, et al. Is body weight the most appropriate criterion to select patients eligible for low-dose pulmonary CT angiography? Analysis of objective and subjective image quality at 80 kVp in 100 patients. *European Radiology* 2009;**19**:1914-22.

27 Nam JM. Testing the Intraclass Version of Kappa Coeffcient of Agreement with Binary Scale and Sample Size Determination. *Biometrical Journal* 2002;**44**:558-570.

28 Cicchetti DV, Feinstein AR. High agreement but low kappa: II. Resolving the paradoxes. *Journal of Clinical Epidemiology* 1990;**43**:551-8.

29 Feinstein AR, Cicchetti DV. High agreement but low kappa: I. The problems of two paradoxes. *Journal of Clinical Epidemiology* 1990;**43**:543-9.

30 Mieville FA, Berteloot L, Grandjean A et al. Model-based iterative reconstruction in pediatric chest CT: assessment of image quality in a prospective study of children with cystic fibrosis. *Pediatric Radiology* 2013;**43**:558-67.

31 Friedman AC, Fiel SB, Fisher MS, et al. Asbestos-related pleural disease and asbestosis: a comparison of CT and chest radiography. *AJR. American Journal of Roentgenology* 1988;**150**:269-75.

32 Ross RM. The clinical diagnosis of asbestosis in this century requires more than a chest radiograph. *Chest* 2003;**124**:1120-8.

33 Green FH, Harley R, Vallyathan V et al. Exposure and mineralogical correlates of pulmonary fibrosis in chrysotile asbestos workers. *Occupational and Environmental Medicine* 1997;**54**:549-59.

34 Paris C, Benichou J, Raffaelli C et al. Factors associated with early-stage pulmonary fibrosis as determined by high-resolution computed tomography among persons

occupationally exposed to asbestos. *Scandinavian Journal of Work, Environment and Health* 2004;**30**:206-14.

35 MacMahon H, Austin JH, Gamsu G et al. Guidelines for management of small pulmonary nodules detected on CT scans: a statement from the Fleischner Society. *Radiology* 2005;**237**:395-400.

Table 1 Subjective noise assessment

	Axial mediastinum		Axial parenchyma		Coronal mediastinum		Coronal parenchyma	
	Veo	FBP	*Veo*	FBP	*Veo*	FBP	*Veo*	FBP
Reader 1								
Minimal, no (%)	2 (7)	22 (82)	6 (21)	25 (93)	19 (68)	25 (93)	22 (79)	26 (96)
Moderate, no (%)	19 (68)	5 (18)	18 (64)	2 (7)	8 (32)	2 (7)	5 (21)	1 (4)
Important, no (%)	6 (25)	0	3 (14)	0	0	0	0	0
P value	**<0.001**		**<0.001**		**0.03**		0.10	
Reader 2								
Minimal, no (%)	2 (7)	17 (64)	4 (14)	26 (96)	8 (29)	19 (68)	19 (68)	26 (96)
Moderate, no (%)	14 (50)	10 (36)	18 (64)	1 (4)	17 (61)	7 (29)	8 (32)	1 (4)
Important, no (%)	11 (43)	0	5 (21)	0	2 (11)	1 (4)	0	0
P value	**<0.001**		**<0.001**		**0.02**		**<0.01**	

Table 2 Objective noise and Signal to Noise Ratio measurements

	Objective noise				Signal to Noise Ratio			
	Veo mean±SD	FBP mean±SD	P value	Decrease (%)	*Veo* mean±SD	FBP mean±SD	P value	Increase (%)
Trachea								
Axial	20.1±3.6	26.1±9.3	**<0.01**	-23	47.5±7.8	42.5±10.9	**0.04**	12
Coronal	21.1±3.4	24.4±7.1	**0.02**	-13	45.7±7.3	43.4±9.7	0.24	5
Descending aorta								
Axial	20.1±3.2	25.1±5.4	**<0.001**	-20	1.7±0.6	1.3±0.3	**<0.001**	33
Coronal	19.8±3.3	24.5±4.5	**<0.001**	-19	1.6±0.6	1.3±0.3	**<0.01**	22
Lung								
Axial	25.8±5.1	32.8± 14.4	**0.02**	-21	34.1±6.6	31.6±10.5	0.25	8
Coronal	27.2±6.1	34.3±10.5	**<0.001**	-21	32.3±7.3	28.5±6.9	**0.03**	13

Table 3 Low dose CT scan with *Veo* reconstruction, accuracy for interstitials abnormalities

	P	τ	κ	Se (CI95%)	Sp (CI95%)	PPV (CI95%)	PNV (CI95%)
Total	**55.6%**	**70.4%**	**0.44**	**46.7%** (21.3-73.4)	**100%** (73.5-100)	**100%** (59-100)	**60%** (36.1-80.9)
Subpleural dots and branching opacities	**33.3%**	**74%**	**0.34**	**33.3%** (7.5-70.1)	**94.4%** (72.7-99.9)	**75%** (19.4-99.4)	**73.9%** (51.6-89.8)
Curvilinear subpleural lines	**8%**	**0**	**0**	**0**	**0**	**0**	**0**
Areas of ground glass opacities	**25.9%**	**77.8%**	**0.2**	**14.3%** (0.4-57.9)	**100%** (83.2-100)	**100%** (2.5-100)	**76.9%** (56.4-91)
Honeycombing	**0**						
Reticulations	**18.5%**	**92.6%**	**0.71**	**60%** (14.7-94.7)	**100%** (84.6-100)	**100%** (29.2-100)	**91.7%** (73-99)
Septal lines	**14.8%**	**85.2%**	**0.26**	**25%** (0.6-80.6)	**95.7%** (78.1-99.9)	**50%** (1.3-98.7)	**88%** (68.8-97.5)

P: prevalence, τ: Agreement with standard CT scan, κ: kappa coefficient, Se: sensitivity, Sp: specificity, PPV: Positive Predictive Value, PVN: Predictive Negative value.

Comparison of the ultra-low-dose *Veo* algorithm with the gold standard filtered back projection for detecting pulmonary asbestos-related conditions: a clinical observational study

Marielle Tekath[1], Frédéric Dutheil[2,3,4,5], Romain Bellini[6], Antoine Roche[1], Bruno Pereira[7], Geraldine Naughton[3,*], Alain Chamoux[2], Jean-Luc Michel[1]

[1] Department of Radiology, University Hospital CHU G. Montpied, Clermont-Ferrand, France

[2] Occupational Medicine, University Hospital CHU G. Montpied, Clermont-Ferrand, France

[3] School of Exercise Science, Australian Catholic University, Locked Bag 4115, Fitzroy MDC, VIC 3065, Australia

[4] Laboratory of Metabolic Adaptations to Exercise in Physiological and Pathological conditions EA3533, Blaise Pascal University, Clermont-Ferrand, France

[5] INRA, UMR 1019, UNH, CRNH Auvergne, Clermont-Ferrand, France

[6] Department of Radiology, Centre Jean Perrin, University Hospital CHU Clermont-Ferrand, France

[7] Department of Medical Statistics, University Hospital CHU G. Montpied, Clermont-Ferrand, France

*** Correspondance to**: Geraldine Naughton; Geraldine.Naughton@acu.edu.au

Running title: *Veo* in asbestos-related conditions

Words count for introduction methods results discussion and conclusion: 2946

Number of tables: 3

Number of figures: 2

Words count for abstract: 249

ABSTRACT

Objectives: Radiation delivered during computed tomography is a major concern, especially for individuals undergoing repeated screening. We aimed to compare a new ultra-low dose algorithm called *Veo* with the gold standard filtered back projection (FBP) for detecting pulmonary asbestos-related conditions.

Setting: University Hospital CHU G. Montpied, Clermont-Ferrand, France

Participants: Asbestos-exposed workers were recruited following referral to screening for asbestos-related conditions. Two acquisitions were performed on a 64-slice computed tomography: the gold standard FBP followed by *Veo* reconstruction.

Outcome measures: Two radiologists independently assessed asbestos-related abnormalities, pulmonary nodules, radiation doses, and image quality (noise).

Results: We included 27 asbestos-exposed workers (63.3±6.5 years with 11.9±9.7 years of asbestos-exposure). We observed 297 pleural plaques in 20 participants (74%). All patients (100%) had pulmonary nodules, totaling 167 nodules. Detection rates did not differ for pleural plaques (*Veo* 87% vs. FBP 97%, NS), pleural thickening (100% for both) and pulmonary nodules (80% for both). Interstitial abnormalities were depicted less frequently with *Veo* than FBP. False negative and false positive did not exceed 2.7%. Compared with FBP, *Veo* decreased the radiation dose up to 87% (*Veo* 0.23±0.07 vs. FBP 1.83±0.88 mSv, $p<0.001$). The objective image noise also decreased with *Veo* as much as 23% and signal to noise ratio increased up to 33%.

Conclusion: A low dose computed tomography with *Veo* reconstruction substantially reduced radiation. *Veo* compared favorably with FBP in detecting pleural plaques, pleural thickening and pulmonary nodules. ~~However, due to a few false positives and false negatives, *Veo* may be better for following up patients after initial screening with FBP~~ These results should be confirmed on a larger sample size before the use of *Veo* in clinical routine practice~~,~~ in asbestos-related conditions, especially regarding the low prevalence of interstitial abnormalities in this study (ClinicalTrials.gov number: NCT01955018).

Formatted: Line spacing: Exactly 25 pt

Formatted: Font: 12 pt

Formatted: Font: Italic

Keywords computed tomography, radiation, screening, asbestos, workers, cancer

Strengths and limitations of this study

- Radiation delivered during computed tomography is a major concern, especially for individuals undergoing repeated screening, such as asbestos-exposed workers.
- We provides the first comparison of a new ultra-low dose algorithm called *Veo* ("I see" in Spanish) with the gold standard filtered back projection (FBP) in detecting pulmonary conditions in asbestos-exposed workers.
- *Veo* substantially reduces radiation doses, with 87% less radiation delivered than FBP.
- *Veo* compared favorably with FBP acquisitions in detecting pleural plaques, diffuse pleural thickening and pulmonary nodules; t~~; however, due to a few false positives and false negatives, *Veo* may be better for following up asbestos-exposed workers after initial screening with FBP.~~
- ~~Even if the sample size could be perceived as a limitation, t~~he high prevalence of pleural plaques (297, observed in 74% of participants) and pulmonary nodules (167) permitted a robust statistical analysis.
- However, ~~-~~these results should be confirmed on a larger sample size before the use of *Veo* in clinical routine practice in asbestos-related conditions, especially regarding the low prevalence of interstitial abnormalities.

Formatted: Font: Italic

INTRODUCTION

Asbestos fibers were intensively used throughout the 20th century [1], and remain prevalent in developing countries.[1] However, asbestos exposure induces a variety of benign and malignant pleural and lung diseases.[2 3] Due to a long latency period between exposure and disease presentation, asbestos-related diseases remain a substantial public health problem.[1] The most common asbestos-induced neoplasm is lung cancer.[2 3] Chest computed tomography (CT) screening has been successfully used in the early detection of lung cancer in asbestos-exposed workers.[4-6] Moreover, thin-section CT is more sensitive than a chest x-ray for detecting early asbestos-related conditions.[7-10] Nevertheless, the use of CT has two main disadvantages: high radiation doses and depiction of incidental abnormalities such as pulmonary nodules in asymptomatic patients. Incidental abnormalities increase the frequency of follow-up by CT and may also psychologically impact on patients. Medical exposure from x-rays represents the major source of man-made irradiation with a large contribution from CT.[11-13] Increased exposure to radiation underpins the consequences of cancer induction.[14] However, reducing CT doses increases image noise from the filtered back projection (FBP) reconstruction. Strategies to reduce radiation exposure include the use of iterative reconstruction algorithms such as "iDose", "100% ASIR" and "IRIS".[15-20] The new algorithm called *Veo*™ (General Electric Healthcare, Milwaukee, MI, USA) decreases the image noise up to 70% compared with the gold standard FBP model, whereas the "100% ASIR" algorithm is only capable of reducing image noise up to 47%.[21] Moreover, *Veo* ("I see" in Spanish) improves spatial resolution with excellent detection of low and high contrast objects from a CT Dose Index ($CTDI_{vol}$) equal to 0.3 mGy.

Thus, the objective of the present study was to compare *Veo* with the gold standard FBP for detecting pulmonary asbestos-related conditions among workers previously exposed to asbestos. Comparisons included radiation delivered and image quality.

Field Code Changed
Field Code Changed
Field Code Changed
Field Code Changed
Field Code Changed
Field Code Changed
Field Code Changed
Field Code Changed
Field Code Changed
Field Code Changed
Field Code Changed

METHODS

Patients

Our ~~prospective~~ clinical observational study received approval from the ethical committee of the University Hospital of Clermont-Ferrand (ClinicalTrials.gov number: NCT01955018). Written informed consent was obtained from all participants for the supplementary acquisition of *Veo* images in addition to their clinically indicated chest CT. Asbestos-exposed workers were recruited following referral to our radiology department for the evaluation of asbestos-related disease between September 2012, and April 2013. Inclusion criteria were being an asbestos-exposed workers, having a chest CT referral from the occupational medicine department, no history of cancer or thoracic surgery, and the absence of other known interstitial pathology.

CT protocol

CT examinations were performed with a 64-slice CT system (Discovery CT 750HD; GE Healthcare, Milwaukee, WI) and consisted of two successive acquisitions. Each examination, the normal-dose (FBP acquisition) and ultra-low-dose (*Veo* acquisition) spiral CT, was obtained on the entire thorax, at full inspiration with the participant in the supine position. -No intravenous contrast material was administered. In accordance with guidelines, standard acquisition was performed with CT parameters adjusted to the participant's body size, including a tube kilovoltage (kV) of 120 (participants weighing 70 kg or less) and 140 (participants weighing more than 70 kg), with milliamperage (mA) equal to the patient's body weight. The other CT parameters were rotation time 0.5 s and pitch 1.375. Image data were

reconstructed with FBP algorithm. The *Veo* acquisition was performed with constant CT parameters including: a tube voltage of 100 kV, a tube current of 20 mA, pitch of 0.984 and rotation time 0.4 s. Image data were reconstructed with the *Veo* algorithm.

Interpretation of CT Images

Each CT acquisition was viewed independently by two ~~experienced~~ radiologists (2 and ~~to~~ 7 years of experience – Drs RB and AR). The low-dose images with *Veo* reconstruction were interpreted before the standard CT and on separate weeks to minimize recall bias. A third ~~The gold standard CT was established by a second and~~ simultaneous reading of the *Veo* and FBP acquisitions by the more experienced radiologist (AR) ~~to~~ evaluated the concordance ~~detection and characterization~~ of pleuroparenchymal abnormalities between *Veo* and FBP. Because FBP images are benchmark practice, when a lesion was found only on *Veo* images, it was regarded as a false positive.

Pleural and parenchymal abnormalities

According to established criteria,[9 22 23] the following asbestos-related pleural and parenchymal abnormalities were recorded as present or absent. Pleural abnormalities considered were:

- Pleural plaques: pleura thickening with no associated parenchymal abnormality. We recorded for each lesion: localization (side, region: anterolateral, posterolateral, diaphragmatic or mediastinum), thickness, and calcification.

- Diffuse pleural thickening: pleural thickening associated with parenchymal abnormalities such as rounded atelectasis and parenchymal bands.[22]

- Pleural effusion is typically asymptomatic, the fluid may be serous or hemorrhagic.[22]

CT features of asbestosis included: 1) subpleural dots and branching opacities, 2) curvilinear subpleural lines, defined as linear opacity within 1 cm of the pleura and parallel to the inner

Formatted: Font: Italic

Field Code Changed

Field Code Changed

Field Code Changed

Field Code Changed

Field Code Changed

chest wall, 3) areas of ground glass opacities, 4) septal lines and 5) reticulations defined as single or branching lines 1-2 cm in length in the subpleural parenchyma, 6) honeycombing, defined as cystic air spaces with well-defined walls less than 1 cm diameter.

Presence of nodules was also recorded. We noted for each abnormality: localization (side, table position) and nature (non-solid, part-solid, solid or calcified). To increase sensitivity, nodules were examined by combining maximum intensity projections and millimetric axial CT images.[24]

Radiation

Comparisons included the dose length product (DLP) in mGy.cm and effective doses in mSv. Computed conversion factor from DLP to effective dose for adult chest is 0.0146 mSv.mGy^{-1}.cm^{-1} [25].

Quality of FBP and *Veo* Images

Respiratory artifacts were graded on a three-point scale (1 = negligible, 2 = moderate, 3 = salient). Images noise was studied in the axial and coronal planes. A similar scale was used for subjective image quality in the mediastinum and parenchyma windows. Objective image noise is the mean of the ~~(~~Standard Deviation~~)~~ of the signal intensity ~~and average CT numbers~~ (in Hounsfield's units) ~~were~~ measured with circular regions of interest (ROI) on different anatomical levels, 10 mm in diameter.[19] ROIs were drawn within the descending thoracic aorta at the level of the left main bronchus, within the tracheal lumen up to the tracheal bifurcation, and on the lung. The signal to noise ratio (SNR) was also calculated using the equation SNR = signal intensity~~CT numbers~~ / objective noise.[26]

Statistical Analysis

Field Code Changed

Field Code Changed

Field Code Changed

Field Code Changed

Sample size estimation was based on the number of pleural plaques and nodules. Considering the investigative nature of the study design and because the number of pleural plaques and nodules was not known initially, a sample size estimation was not proposed *a priori* even though a concordance coefficient kappa (κ) between 0.40 and 0.90 was expected between filtered back projection images and *Veo* images. Therefore, 30 asbestos-exposed workers were predicted to be necessary to reject the null hypothesis "H0: $\kappa = 0.40$" vs. "H1: $\kappa \neq 0.75$" for a proportion of pleural plaques of 65%, with a statistical power of > 85% and α=5% (two-sided). Finally, the study was conducted to sequentially control the statistical power considering the number of plaques and nodules for each asbestos-exposed worker.[27]

Field Code Changed

Statistical analysis was performed using Stata software (version 12; Stata-Corp, College Station, Tex., USA). Quantitative variables are expressed as means ± standard deviations (SD). Proportions are expressed as percentage and 95% confidence intervals (CIs). Comparisons in paired situation were realized using paired Student t-test or Wilcoxon test when appropriate for quantitative variables and Stuart-Maxwell test for categorical parameters. Sensitivity, specificity, false positives and false negatives values of *Veo* were calculated and presented with 95% confidence intervals, in comparison with results from FBP acquisitions. Estimates of sensitivity and specificity were obtained by first estimating the sensitivity and specificity for each patient. Sensitivity and specificity were then estimated by averaging the individual specific estimates across patients. The variance of the estimate was the sample variance divided by the number of patients. Generalized estimating~~ed~~ equation models with logit link and working independence correlation structure were also used to estimate sensitivity, taking into account the correlation among the multiple pleural plaques and pulmonary nodules for the same patient. The kappa coefficient was used to measure agreement for categorical parameters and Pearson's correlation coefficient and Lin concordance correlation coefficient for quantitative data. The analyses were completed by

using of random-effect models when appropriate to consider within and between participant variability. The tests were two-sided, with a type I error set at α=0.05.

RESULTS

Patients

The flow chart of participants is displayed in Figure 1. Among the 87 asbestos-exposed workers referred to our radiology department, 29 gave their consent and, 27 were retained for analyses. The mean age of volunteers was 63.3±6.5 years old. The mean duration of occupational exposure was 11.9±9.7 years.

Radiation dose

The average DLP was 16±5 mGy.cm for *Veo* and 125±61 mGy.cm for FBP. The corresponding average effective doses were 0.234±0.073 mSv for *Veo* and 1.825±0.876 mSv for FBP. The dose reduction was calculated to be 87.2% (p<0.001).

Quality images assessment

For *Veo* acquisition, respiratory artifacts were graded as "negligible" in 24 cases (89%) for reader 1 and 25 cases (93%) for reader 2, "moderate" in 3 cases (11%) for reader 1 and 2 cases (7%) for reader 2, and no "salient" artifact was recorded. For FBP acquisition, respiratory artifacts were graded as "negligible" in 19 cases (70%) for reader 1 and 24 cases (89%) for reader 2, "moderate" in 7 cases (26%) for reader 1 and 3 cases (11%) for reader 2, and as "salient" in 1 case for reader 1 and in 0 cases for reader 2. *Veo* and FBP did not differ

in subjective assessment of respiratory artifacts between the two radiologists (p=0.16 for reader 1 and p=0.65 for reader 2).

Tables 1 and 2 provide results from *subjective* image noise assessed by the two radiologists using, average of objective noise data and SNR. The two protocols differed significantly in *objective* image noise. The ultra-low-dose *Veo* acquisition reduced objective image noise from 13 to 23% and increased SNR from 5 to 33% compared with the standard FBP acquisition.

However, the two readers rated higher *subjective* image noise ~~rated higher by the two readers~~ in axial and coronal planes with *Veo* than FBP, with the exception of parenchymal analysis in the coronal plane for the reader 1 (Table 1).

Pleural plaques

A total of 297 pleural plaques (Figure 2) were observed in 20 participants (74%). Detection of plaques did not differ between *Veo* (259; 87%) and FBP (287; 97%) (p=0.10). Thus, the third simultaneous reading of *Veo* and FBP resulted in the detection of 10 plaques that were not detected during the first reading of FBP images. The agreement for pleural plaques depiction was 84% with a kappa of 0.05. However, when data were examined only for the presence of pleural plaque (yes or no) in patients, agreement increased to 96% (κ = 0.91).[28 29] Moreover agreement for size measurement (Lin coefficient) was 0.83 (p<0.001) and k coefficient for calcification detection was 0.86.

For one participant, despite a *Veo* acquisition considered normal, FBP acquisition was positive for one isolated plaque.

Simultaneous analysis of *Veo* and FBP acquisitions led us to observe that *Veo* acquisition was responsible for 3 false positives corresponding to intercostal fat or muscles, with 8 false negatives (2.7%).

Formatted: Font: Not Italic

Formatted: Font: Italic

Field Code Changed

Field Code Changed

Pleural thickening

Diffuse pleural thickening (Figure 2) was present in four patients (14.8%). The detection rate for each technique was 100% with a kappa of 1. No pleural effusion was found.

Parenchymal abnormalities

Parenchymal changes were found in 15 participants (55.6%), including subpleural dots, curvilinear subpleural lines, ground glass opacities, septal lines and reticulations. No honeycombing was found. Table 3 summarizes the prevalence (P), inter-rater agreement (τ) and kappa κ between *Veo* and FBP acquisition, and the sensitivity, specificity, predictive positive value and predictive negative value of *Veo* acquisition for each interstitial abnormality.

Pulmonary nodules

Pulmonary nodules (Figure 2) were found in all patients, with a total of 167 nodules. All the nodules detected were smaller than 10 mm. No non-solid or part-solid nodules were observed. Among the 167 recorded nodules, the detection rate did not differ (p = 0.98) between *Veo* (134/167) and standard FBP (133/167), with the same 80% detection rate. Thus, the third simultaneous reading of *Veo* and FBP resulted in the detection of 34 nodules that were not detected during the first reading of FBP images.-.The agreement between the two techniques for nodules depiction was 60% (κ = 0.25). Simultaneous analysis of *Veo* and FBP acquisitions permitted ~~led~~ us to observe that *Veo* acquisition was responsible for seven false positives (4%) and four false negatives (2.7%).

Inter-observer agreement

No difference was observed for the inter-observer agreement (kappa) between the two techniques. Inter-observer agreement was low for pleural plaques detection (0.09 for FBP and 0.10 for *Veo*) and fair for nodule detection (0.34 for FBP and 0.34 for *Veo*). The inter-reader agreements for parenchymal interstitial abnormalities and parenchymal diffuse pleural thickening were not evaluated due to their low prevalence.

DISCUSSION

We compared for the first time low-dose CT using *Veo* reconstruction and the gold standard CT using FBP reconstruction to depict asbestos-related abnormalities and pulmonary nodules depiction. The major finding was that *Veo* compared favorably with FBP acquisitions in detecting pleural plaques, diffuse pleural thickening and pulmonary nodules. However, interstitial parenchymal abnormalities were depicted less frequently in *Veo* than FBP acquisitions. Nevertheless, *Veo* delivered 87% less radiation than FBP.

Quality of images

The assessment of image quality showed discordant results. Despite low scanning parameters, the iterative reconstruction method of *Veo* significantly reduced the level of objective noise, but subjective noise parameters increased in comparison with FBP. This discordance may be explained by the novel appearance of *Veo* images requiring adaptation time for the radiologists. Our results are in line -with previous results showing a relative noise reduction of 25% obtained from *Veo* (100 kV, 10 mAs) compared with FBP protocol (100 kV, 50-300 mAs).[30]

Field Code Changed

Pleural plaques

Pleural plaques corresponding to parietal pleura fibrosis are indicators of asbestos-exposure [7] with a prevalence as high as 60% in previously exposed workers [10 31] and 74% in the current study with highly exposed workers. In France, the detection of pleural plaques results in financial compensation for workers and early retirement. Consequently, pleural plaques are accepted only when results are unequivocal. Atypical plaques will only be considered when they occur bilateraly or in multiple sites, and with typical localization. Due to the three cases of false positive and 8 cases of false negative, the low dose CT with *Veo* reconstruction cannot be used for the first examination, but its use seems possible for patients' follow-up.

Diffuse pleural thickening detection

Our results indicated that a low dose scanner with *Veo* reconstruction was comparable with the FBP gold standard for diffuse pleural thickening detection. The prevalence of thickening was rare thus, we could not obtain statistical significance. However, thickening remains of major importance because diagnosis results not only in compensation, but guarantees a life-long pension. Considering the importance usually noted about these lesions, a *Veo* acquisition should be sufficient in clinical practice.

Parenchymal abnormalities

Reader sensitivity with *Veo* images was poor for interstitial parenchymal abnormalities. No case of true asbestosis was recorded, but 15 patients had non-specific interstitial abnormalities. However, the detection of interstitial abnormalities may be limited by several factors. First, the study was built for asbestos-related diseases. Recording specifications lacked the details required to comprehensively describe the presence of interstitial abnormalities. Therefore, without systematic records, interstitial abnormalities were likely

Field Code Changed

Field Code Changed

Field Code Changed

underestimated. Second, *Veo* was always performed after FBP resulting in an increase of gravity-dependent attenuation in the posterior region which may have masked interstitial abnormalities. Third, the acquisitions were performed in the supine position and acquisitions in the prone position were not always performed when necessary. Subsequently, the posterior region was not analyzed with confidence. Thus, interstitials abnormalities were underestimated in our study.

Asbestosis refers to interstitial fibrosis caused by the deposition of asbestos fibers in the lung. Its prevalence is estimated to be about 5% in asbestos exposed workers.[32] Asbestosis remains difficult to diagnose, particularly in early stages. However, a significant dose-effect relationship exists between the cumulative exposure to asbestos and asbestosis.[33] Asbestosis is usually associated with dyspnea, basilar rales, and changes in pulmonary function with restrictive or mixed restrictive-obstructive patterns, and carbon monoxide diffusion abnormalities. Pulmonary asbestosis was previously diagnosed in 51 of 706 (7%) of asbestos-exposed workers.[34] In a previous study, 51 of the 706 (7%) of asbestos-exposed workers were diagnosed with pulmonary asbestosis. In this study, only 2% of the workers with less than 25 years of cumulative exposure to asbestos were diagnosed with asbestosis using high resolution CT screening.[34] Therefore, CT screening for asbestosis does not seem warranted in workers with low occupational exposure.

Pulmonary nodules

In our study, all individuals had at least one pulmonary nodule. FBP and *Veo* shared the same detection rate of 80%. However, *Veo* reconstruction is not advised for initial nodules screening due to the 7 false positives and 4 false negatives from the 167 nodules. According to the Fleischner Society guidelines[35], nodule detection on CT requires specific management. In agreement with our recommendations for pleural plaques detection, *Veo* should be used

Field Code Changed

Field Code Changed

Field Code Changed

Field Code Changed

Field Code Changed

only for patients' follow-up after a first detection of pulmonary nodules using gold standard CT.

Comparison of *Veo* with other low-dose algorithms

To date, no studies using other algorithms to reduce radiation exposure have investigated asbestos-related conditions. Thus, because the *Veo* algorithm appears to reduce the more radiation delivered than other low-dose algorithm such as "iDose", "100% ASIR" or "IRIS"[15-20], we chose only to compare *Veo* with the gold standard FBP.

Formatted: Font: Italic

Formatted: Font: Italic

Formatted: Font: Italic

Limitations

The sample size could be perceived as a limitation. Limited sample size exacerbated the need for rapid adaptation time by the radiologists with relatively novel images. However, statistically, the high prevalence of pleural plaques (297, observed in 74% of participants) and pulmonary nodules (167) permitted a robust statistical analysis. Considering these results ($\kappa = 0.91$), power seemed satisfactory (80%) to reject the null hypothesis "H0: $\kappa = 0.4$" vs. "H1: $\kappa \neq 0.91$" with 27 patients. In contrast, parenchymal interstitial abnormalities were rare, precluding sound statistical analyses. Parenchymal interstitial abnormalities suffered from majors limitations due to CT positioning of patients. A further study dedicated to parenchymal interstitial abnormalities should be conducted. Clinically, a current limitation of iterative reconstruction is a long computing time.

CONCLUSION

A low dose computed tomography with *Veo* reconstruction substantially reduces radiation. Despite an unusual appearance, *Veo* image quality was generally accurate in its diagnosis.

Specifically, *Veo* compared favorably with the gold standard filtered back projection acquisitions in detecting pleural plaques, diffuse pleural thickening and pulmonary nodules. However, ~~due to a few false positives and false negatives, *Veo* may be best used for follow up of patients after initial screening with filtered back projection.~~these results should be confirmed on a larger sample size before the use of *Veo* in clinical routine practice in asbestos-related conditions, especially regarding the low prevalence of interstitial abnormalities in this study.

Formatted: Font: Italic

Funding The study was funded by the University Hospital CHU G. Montpied, 58 rue Montalembert 63000 Clermont-Ferrand, France. The funders had no role in study design, data collection and analysis, decision to publish, or preparation of the manuscript.

Contributors MT has participated as a MD student and principal investigator. MT, FD, AC and JLM obtained research funding and generated the intellectual development of the study. MT and FD obtained the ethics approval. FD and AC recruited all participants. RB and AR completed the double blind analyses of *Veo* and FBP images. MT and BP made data analysis. MT drafted the manuscript. FD and GN revised the manuscript. All authors read and approved the final manuscript.

Formatted: Font: Italic

Acknowledgments Our thanks to the "CAPER des Combrailles" (Association of the asbestos-exposed workers), which helped us recruit the asbestos-exposed workers.

Competing interests None.

Ethics approval Approval was given by the regional ethics committee (ClinicalTrials.gov number: NCT01955018).

Data sharing statement Original data from this study are available by contacting the corresponding author via email.

REFERENCES

1 Stayner L, Welch LS, Lemen R. The worldwide pandemic of asbestos-related diseases. *Annual Review of Public Health* 2013;**34**:205-16.

2 Oksa P, Pukkala E, Karjalainen A, Ojajarvi A, Huuskonen MS. Cancer incidence and mortality among Finnish asbestos sprayers and in asbestosis and silicosis patients. *American Journal of Industrial Medicine* 1997;**31**:693-8.

3 Koskinen K, Pukkala E, Martikainen R, Reijula K, Karjalainen A. Different measures of asbestos exposure in estimating risk of lung cancer and mesothelioma among construction workers. *Journal of Occupational and Environmental Medicine* 2002;**44**:1190-6.

4 Clin B, Morlais F, Guittet L et al. Performance of chest radiograph and CT scan for lung cancer screening in asbestos-exposed workers. *Occupational and Environmental Medicine* 2009;**66**:529-34.

5 Fasola G, Belvedere O, Aita M et al. Low-dose computed tomography screening for lung cancer and pleural mesothelioma in an asbestos-exposed population: baseline results of a prospective, nonrandomized feasibility trial--an Alpe-adria Thoracic Oncology Multidisciplinary Group Study (ATOM 002). *The Oncologist* 2007;**12**:1215-24.

6 Vierikko T, Jarvenpaa R, Autti T et al. Chest CT screening of asbestos-exposed workers: lung lesions and incidental findings. *European Respiratory Journal* 2007;**29**:78-84.

7 American Thoracic Society. Diagnosis and initial management of nonmalignant diseases related to asbestos. *American Journal of Respiratory and Critical Care Medicine* 2004;**170**:691-715.

8 Akira M, Yamamoto S, Yokoyama K et al. Asbestosis: high-resolution CT-pathologic correlation. *Radiology* 1990;**176**:389-94.

9 Akira M, Yokoyama K, Yamamoto S et al. Early asbestosis: evaluation with high-resolution CT. *Radiology* 1991;**178**:409-16.

10 Neri S, Antonelli A, Falaschi F, Boraschi P, Baschieri L. Findings from high resolution computed tomography of the lung and pleura of symptom free workers exposed to amosite who had normal chest radiographs and pulmonary function tests. *Occupational and Environmental Medicine* 1994;**51**:239-43.

Field Code Changed

Formatted: Font: Times New Roman, 12 pt

Formatted: Font: Times New Roman, 12 pt, French (France)

Formatted: Font: Times New Roman, 12 pt

11 Mettler FA, Jr., Thomadsen BR, Bhargavan M et al. Medical radiation exposure in the U.S. in 2006: preliminary results. *Health Physics* 2008;**95**:502-7.
12 Samara ET, Aroua A, Bochud FO et al. Exposure of the Swiss population by medical x-rays: 2008 review. *Health Physics* 2012;**102**:263-70.
13 Shrimpton PC, Hillier MC, Lewis MA, Dunn M. National survey of doses from CT in the UK: 2003. *British Journal of Radiology* 2006;**79**:968-80.
14 Brenner DJ, Hall EJ. Computed tomography--an increasing source of radiation exposure. *New England Journal of Medicine* 2007;**357**:2277-84.
15 Marin D, Nelson RC, Schindera ST et al. Low-tube-voltage, high-tube-current multidetector abdominal CT: improved image quality and decreased radiation dose with adaptive statistical iterative reconstruction algorithm--initial clinical experience. *Radiology* 2010;**254**:145-53.
16 Pontana F, Duhamel A, Pagniez J et al. Chest computed tomography using iterative reconstruction vs filtered back projection (Part 2): image quality of low-dose CT examinations in 80 patients. *European Radiology* 2011;**21**:636-43.
17 Pontana F, Pagniez J, Flohr T et al. Chest computed tomography using iterative reconstruction vs filtered back projection (Part 1): Evaluation of image noise reduction in 32 patients. *European Radiology* 2011;**21**:627-35.
18 Ren Q, Dewan SK, Li M et al. Comparison of adaptive statistical iterative and filtered back projection reconstruction techniques in brain CT. *European Journal of Radiology* 2012;**81**:2597-601.
19 Silva AC, Lawder HJ, Hara A, Kujak J, Pavlicek W. Innovations in CT dose reduction strategy: application of the adaptive statistical iterative reconstruction algorithm. *AJR. American Journal of Roentgenology* 2010;**194**:191-9.
20 Singh S, Kalra MK, Gilman MD et al. Adaptive statistical iterative reconstruction technique for radiation dose reduction in chest CT: a pilot study. *Radiology* 2011;**259**:565-73.
21 Mieville FA, Gudinchet F, Brunelle F, Bochud FO, Verdun FR. Iterative reconstruction methods in two different MDCT scanners: physical metrics and 4-alternative forced-choice detectability experiments--a phantom approach. *Phys Med* 2013;**29**:99-110.
22 Gevenois PA, de Maertelaer V, Madani A, Winant C, Sergent G, De Vuyst P. Asbestosis, pleural plaques and diffuse pleural thickening: three distinct benign responses to asbestos exposure. *European Respiratory Journal* 1998;**11**:1021-7.
23 Roach HD, Davies GJ, Attanoos R, Crane M, Adams H, Phillips S. Asbestos: when the dust settles an imaging review of asbestos-related disease. *Radiographics* 2002;**22 Spec No**:S167-84.
24 Jankowski A, Martinelli T, Timsit JF et al. Pulmonary nodule detection on MDCT images: evaluation of diagnostic performance using thin axial images, maximum intensity projections, and computer-assisted detection. *European Radiology* 2007;**17**:3148-56.
25 Deak PD, Smal Y, Kalender WA. Multisection CT protocols: sex- and age-specific conversion factors used to determine effective dose from dose-length product. *Radiology* 2010;**257**:158-66.
26 Szucs-Farkas Z, Strautz T, Patak MA, Kurmann L, Vock P, Schindera ST. Is body weight the most appropriate criterion to select patients eligible for low-dose pulmonary CT angiography? Analysis of objective and subjective image quality at 80 kVp in 100 patients. *European Radiology* 2009;**19**:1914-22.
27 Nam JM. Testing the Intraclass Version of Kappa Coeffcient of Agreement with Binary Scale and Sample Size Determination. *Biometrical Journal* 2002;**44**:558-570.

Formatted: Font: Times New Roman, 12 pt, French (France)

Formatted: Font: Times New Roman, 12 pt

28 Cicchetti DV, Feinstein AR. High agreement but low kappa: II. Resolving the paradoxes. *Journal of Clinical Epidemiology* 1990;**43**:551-8.

29 Feinstein AR, Cicchetti DV. High agreement but low kappa: I. The problems of two paradoxes. *Journal of Clinical Epidemiology* 1990;**43**:543-9.

30 Mieville FA, Berteloot L, Grandjean A et al. Model-based iterative reconstruction in pediatric chest CT: assessment of image quality in a prospective study of children with cystic fibrosis. *Pediatric Radiology* 2013;**43**:558-67.

31 Friedman AC, Fiel SB, Fisher MS, Radecki PD, Lev-Toaff AS, Caroline DF. Asbestos-related pleural disease and asbestosis: a comparison of CT and chest radiography. *AJR. American Journal of Roentgenology* 1988;**150**:269-75.

32 Ross RM. The clinical diagnosis of asbestosis in this century requires more than a chest radiograph. *Chest* 2003;**124**:1120-8.

33 Green FH, Harley R, Vallyathan V et al. Exposure and mineralogical correlates of pulmonary fibrosis in chrysotile asbestos workers. *Occupational and Environmental Medicine* 1997;**54**:549-59.

34 Paris C, Benichou J, Raffaelli C et al. Factors associated with early-stage pulmonary fibrosis as determined by high-resolution computed tomography among persons occupationally exposed to asbestos. *Scandinavian Journal of Work, Environment and Health* 2004;**30**:206-14.

35 MacMahon H, Austin JH, Gamsu G et al. Guidelines for management of small pulmonary nodules detected on CT scans: a statement from the Fleischner Society. *Radiology* 2005;**237**:395-400.

Table 1 Subjective noise assessment

	Axial mediastinum		Axial parenchyma		Coronal mediastinum		Coronal parenchyma	
	Veéo	FBP	*Veéo*	FBP	*Veéo*	FBP	*Veéo*	FBP
Reader 1								
Minimal, no.(%)	2 (7)	22 (82)	6 (21)	25 (93)	19 (68)	25 (93)	22 (79)	26 (96)
Moderate, no.(%)	19 (68)	5 (18)	18 (64)	2 (7)	8 (32)	2 (7)	5 (21)	1 (4)
Important, no.(%)	6 (25)	0	3 (14)	0	0	0	0	0
P value	**<0.001**		**<0.001**		**0.03**		0.10	
Reader 2								
Minimal, no.(%)	2 (7)	17 (64)	4 (14)	26 (96)	8 (29)	19 (68)	19 (68)	26 (96)
Moderate, no.(%)	14 (50)	10 (36)	18 (64)	1 (4)	17 (61)	7 (29)	8 (32)	1 (4)
Important, no.(%)	11 (43)	0	5 (21)	0	2 (11)	1 (4)	0	0
P value	**<0.001**		**<0.001**		**0.02**		**<0.01**	

Formatted: Justified, Space After: 10 pt, Line spacing: Double

Formatted Table

Formatted: Font: Italic

Formatted: Font: Italic

Formatted: Font: Italic

Formatted: Font: Italic

Formatted: Font: Bold

Formatted: Font: Bold

Table 2 Objective noise and Signal to Noise Ratio mean values of SD and SNR measurements

	Objective noise				Signal to Noise Ratio			
	Veo (UH) mean±SD	FBP (UH) mean±SD	P value	Decrease (%)	*Veo* mean±SD	FBP mean±SD	P value	Increase (%)
Trachea								
Axial	20.12± (3.62)	26.11± (9.34)	**<0.01**	-23%	47.50± (7.84)	42.548± (10.986)	**0.04**	12
Coronal	21.109± (3.436)	24.347± (7.12)	**0.02**	-13%	45.7± (7.31)	43.439 (±9.765)	0.24	5
Descending aorta								
Axial	20.12± (3.219)	25.12± (5.41)	**<0.001**	-20%	1.67± (0.655)	1.328± (0.32)	**<0.001**	33
Coronal	19.78± (3.32)	24.547± (4.51)	**<0.001**	-19%	1.64± (0.655)	1.34± (0.32)	**<0.01**	22
Lung								
Axial	25.82± (5.10)	32.83± (14.437)	**0.02**	-21%	34.13 ±(6.62)	31.657± (10.549)	0.25	8
Coronal	27.152± (6.14)	34.326 ±(10.45)	**<0.001**	-21%	32.325± (7.30)	28.547± (6.94)	**0.03**	13

Formatted: Font: Not Bold

Formatted Table

Formatted: Font: Bold

Formatted: Font: Bold

Formatted: Font: Bold

Formatted: Font: Bold

Formatted: Font: Bold

Formatted: Font: Bold

Table 3 Low dose CT scan with *Veo* reconstruction, accuractely for interstitials abnormalities

	P	τ	κ	Se (ICI95%)	Sp (ICI95%)	PPV (ICI95%)	PNV (ICI95%)
Total	**55.6%**	**70.437%**	**0.44**	**46.7%** (21.3-73.4)	**100%** (73.5-100)	**100%** (59-100)	**60%** (36.1-80.9)
Subpleural dots and branching opacities	**33.3%**	**74%**	**0.34**	**33.3%** (7.5-70.1)	**94.4%** (72.7-99.9)	**75%** (19.4-99.4)	**73.9%** (51.6-89.8)
Curvilinear subpleural lines	**8%**	**0**	**0**	**0**	**0**	**0**	**0**
Areas of ground glass opacities	**25.9%**	**77.8%**	**0.2**	**14.3%** (0.4-57.9)	**100%** (83.2-100)	**100%** (2.5-100)	**76.9%** (56.4-91)
Honeycombing	**0**						
Réticulations	**18.5%**	**92.6%**	**0.71**	**60%** (14.7-94.7)	**100%** (84.6-100)	**100%** (29.2-100)	**91.7%** (73-99)
Septal lines	**14.8%**	**85.2%**	**0.26**	**25%** (0.6-80.6)	**95.7%** (78.1-99.9)	**50%** (1.3-98.7)	**88%** (68.8-97.5)

P: prevalence, τ: Agreement with standard CT scan, κ: kappa coefficient, Se: sensitivity, Sp: specificity, PPV: Positive Predictive Value, PVN: Predictive Negative value.

Figure 1 Flow-chart of participants.

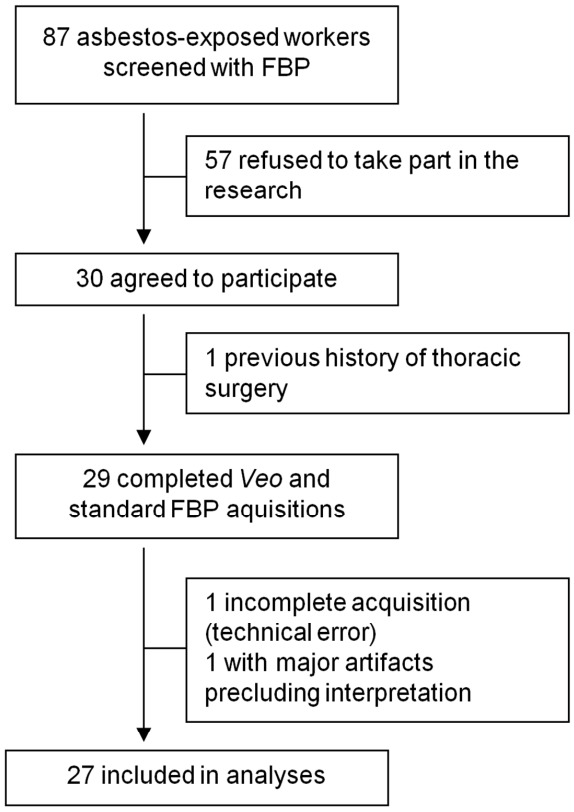

Figure 2 Typical pleural plaques (1. white arrows), diffuse pleural thickening (2. white arrows) and parenchymal band (2. black arrows), and pulmonary nodule (3. white arrows) in axial plane and an example of normal images in axial plane (4). All *Veo* and FBP images are captured at the same anatomic level, with 100 kV and 20 mAs per section for *Veo* and 120 kV, 60 mAs for FBP.

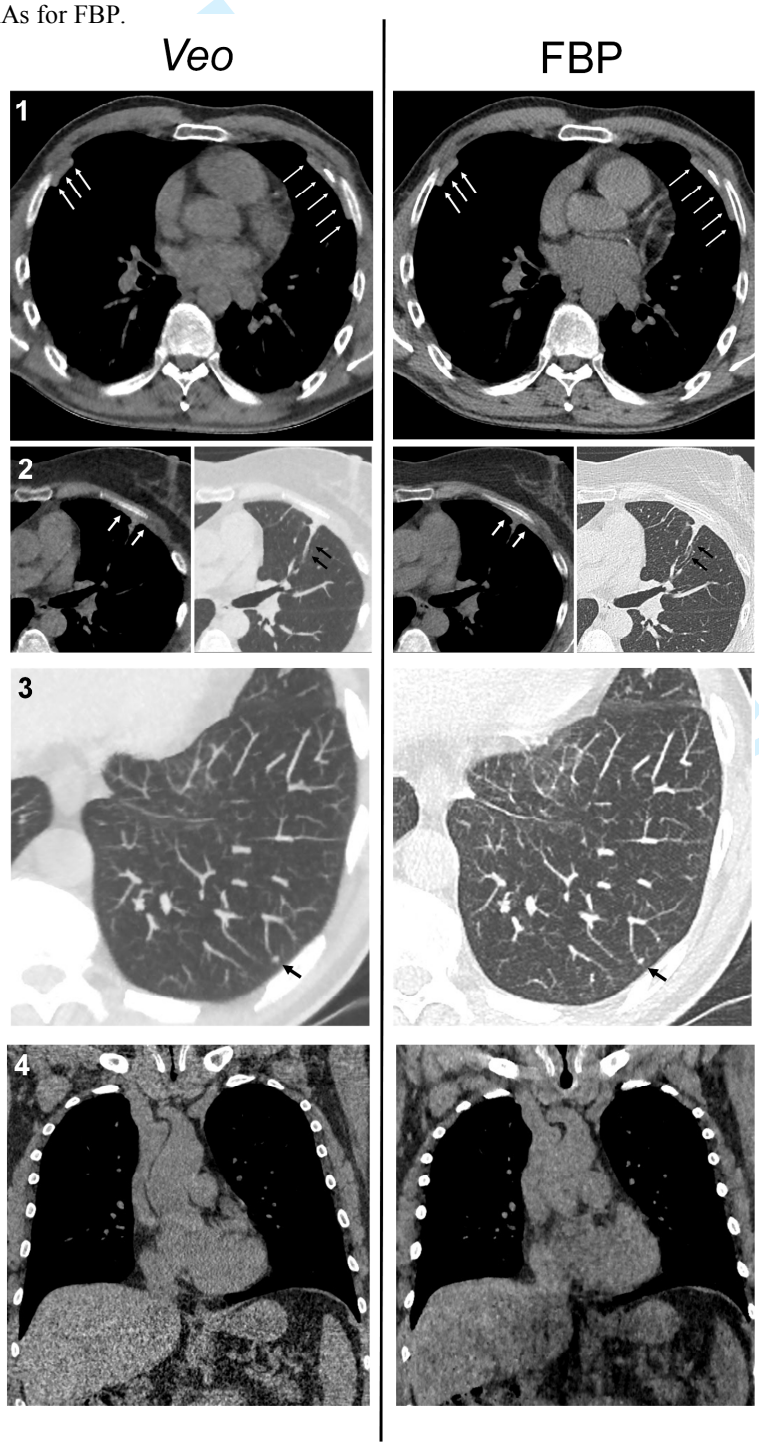

Formatted: Font: Times New Roman, 12 pt, Bold

Formatted: Font: Italic

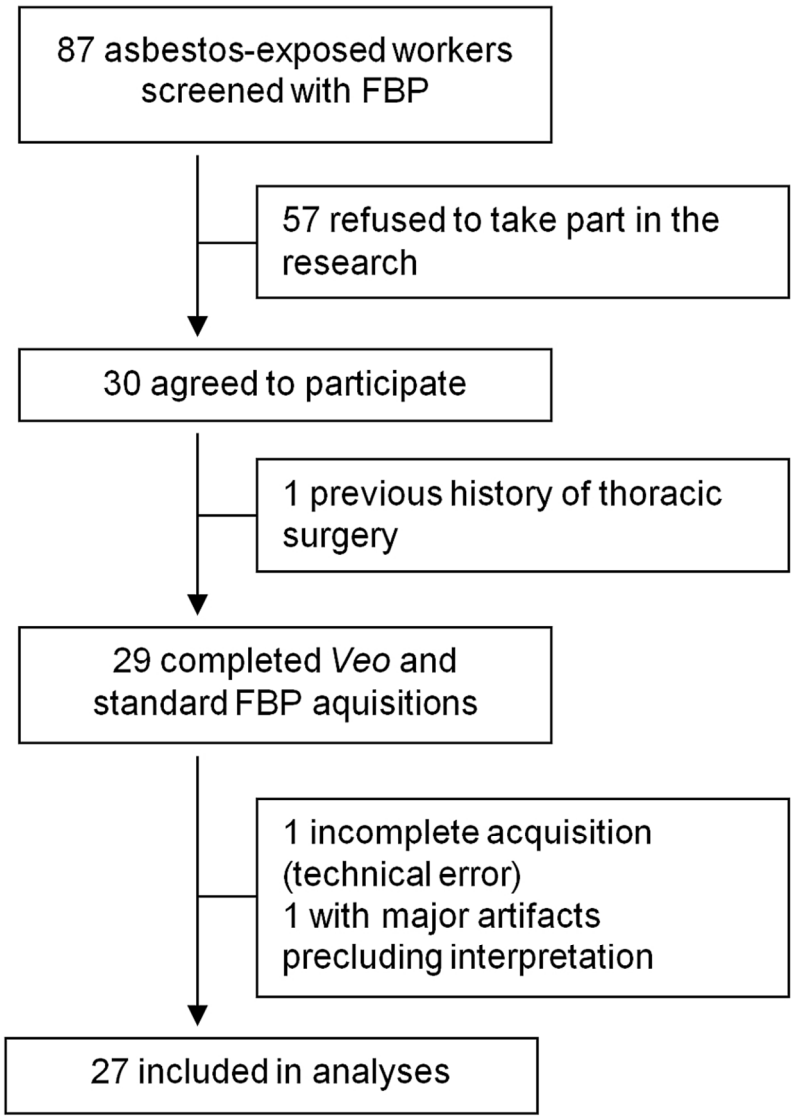

90x119mm (300 x 300 DPI)

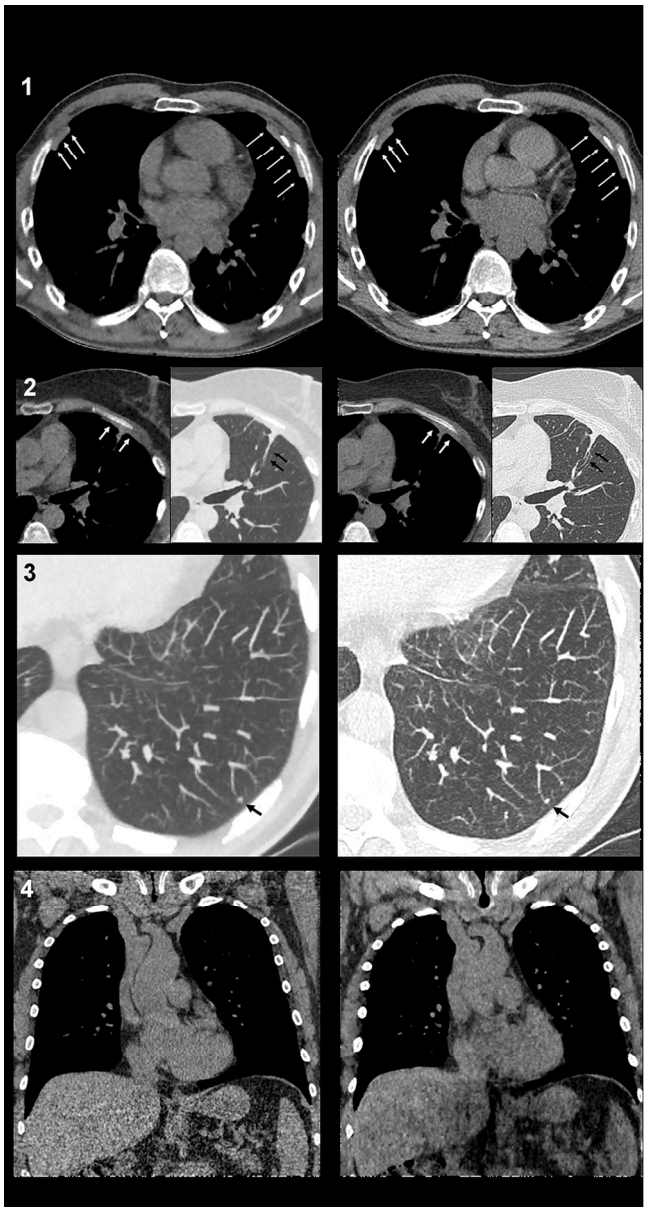

90x169mm (300 x 300 DPI)

STARD checklist for reporting of studies of diagnostic accuracy

(version January 2003)

Section and Topic	Item #		On page #
TITLE/ABSTRACT/ KEYWORDS	1	Identify the article as a study of diagnostic accuracy (recommend MeSH heading 'sensitivity and specificity').	1
INTRODUCTION	2	State the research questions or study aims, such as estimating diagnostic accuracy or comparing accuracy between tests or across participant groups.	3
METHODS			
Participants	3	The study population: The inclusion and exclusion criteria, setting and locations where data were collected.	4
	4	Participant recruitment: Was recruitment based on presenting symptoms, results from previous tests, or the fact that the participants had received the index tests or the reference standard?	4
	5	Participant sampling: Was the study population a consecutive series of participants defined by the selection criteria in item 3 and 4? If not, specify how participants were further selected.	Yes (4)
	6	Data collection: Was data collection planned before the index test and reference standard were performed (prospective study) or after (retrospective study)?	Prospective: see page 4 and stats page 7
Test methods	7	The reference standard and its rationale.	7
	8	Technical specifications of material and methods involved including how and when measurements were taken, and/or cite references for index tests and reference standard.	4 to 6
	9	Definition of and rationale for the units, cut-offs and/or categories of the results of the index tests and the reference standard.	4 to 6
	10	The number, training and expertise of the persons executing and reading the index tests and the reference standard.	Page 5: Interpretation of CT Images
	11	Whether or not the readers of the index tests and reference standard were blind (masked) to the results of the other test and describe any other clinical information available to the readers.	Page 5: Interpretation of CT Images
Statistical methods	12	Methods for calculating or comparing measures of diagnostic accuracy, and the statistical methods used to quantify uncertainty (e.g. 95% confidence intervals).	7
	13	Methods for calculating test reproducibility, if done.	NA
RESULTS			
Participants	14	When study was performed, including beginning and end dates of recruitment.	4: between September 2012, and April 2013
	15	Clinical and demographic characteristics of the study population (at least information on age, gender, spectrum of presenting symptoms).	8
	16	The number of participants satisfying the criteria for inclusion who did or did not undergo the index tests and/or the reference standard; describe why participants failed to undergo either test (a flow diagram is strongly recommended).	8 and figure 3 flow chart
Test results	17	Time-interval between the index tests and the reference standard, and any treatment administered in between.	Simultaneously: see CT protocol pages 6-7
	18	Distribution of severity of disease (define criteria) in those with the target condition; other diagnoses in participants without the target condition.	9-10 if applicable
	19	A cross tabulation of the results of the index tests (including indeterminate and missing results) by the results of the reference standard; for continuous results, the distribution of the test results by the results of the reference standard.	See tables
	20	Any adverse events from performing the index tests or the reference standard.	Impossible to have an adverse event with Veo
Estimates	21	Estimates of diagnostic accuracy and measures of statistical uncertainty (e.g. 95% confidence intervals).	See limitations p14 and p9-10

	22	How indeterminate results, missing data and outliers of the index tests were handled.	Excluded: page 8 and flow chart figure 3
	23	Estimates of variability of diagnostic accuracy between subgroups of participants, readers or centers, if done.	NA
	24	Estimates of test reproducibility, if done.	NA
DISCUSSION	25	Discuss the clinical applicability of the study findings.	Page 13